Supplementary information for:

Does Tafel Analysis Make Sense for Water Oxidation at Metal Oxide/Oxyhydroxide Electrocatalysts?

Wenhua Leng[1*]

Department of Chemistry, Zijingang Campus, Zhejiang University, Hangzhou,

Zhejiang 310058, China

Contents:

[*] Email: lengwh@zju.edu.cn

Supplementary Note 1

Origin of equation 3 in the main text

Theory calculation[1] indicates that the rate-determining inner-sphere reaction step (O–O coupling) for OER involves the reaction between the oxidative charge (Q) in the catalysts and H_2O or OH^-, thus the OER rate would increase with the concentration of the oxidative charges. Also, theory calculation[1] demonstrates that the activation energy (E_a) for O–O coupling obeys the BrØnsted-Evans-Polanyi (BEP) relationship, with E_a depending linearly on a heat of reaction (ΔH_{rxn}), which in turn is controlled by oxidative charge (rather than the capacitive). Thus the E_a for O–O coupling can then be written as **equation S1**, where ζ and κ are constant and the analogues of the BrØnsted-Evans-Polanyi (BEP) slope and intercept, respectively. Inserting this equation into Arrhenius equation produces the rate constant which is therefore oxidative charge density dependent. Thus the rate equation can be written as **equation 3** in the main text and reproduced here (**equation S2**) for convenience, where C_1 is the pre-exponential factor in Arrhenius equation, k_0 is constant and equals $k_0 = C_1 \exp\left(\frac{\kappa}{\kappa_B T}\right)$. Note that electron charge is negative and thus the value of A is positive and equals $q/(\kappa_B T C_a)$.

$$E_a = \zeta Q + \kappa \qquad \textbf{(S1)}$$

$$i = k_{WO} Q = C_1 \exp\left(-\frac{\zeta Q + \kappa}{\kappa_B T}\right) Q = k_0 \exp(qQ/(\kappa_B T C_a)) Q = k_0 \exp(AQ) Q \qquad \textbf{(S2)}$$

Particular note that **equation S2** can be formally written as **equation S3,** where C_H is the Helmholtz capacitance, φ_H is the potential drop across the Helmholtz layer ($\varphi_H = Q/C_H$) and A' equals $q/(\kappa_B T C_H)$. **Equation S3** looks like a Tafel kinetic

equation, which focuses on electron transfer, can only apply to outer-sphere single electron transfer (out-sphere theory, with a large reorganizational energy and neglecting cathodic reaction current, Marcus theory reduces to the Butler–Volmer and thus Tafel equation). This similarity in form can partly explain why models of outer-sphere are capably and commonly applied to inner-sphere electrocatalysis as addressed in details in the main text, though there is the tremendous mechanistic distinction.

$$i = k_0 \exp(qQ/(\kappa_B T C_H))Q = k_0 \exp(q\varphi_H/(\kappa_B T))Q = k_0 \exp(A'Q)Q \qquad \textbf{(S3)}$$

Supplementary Note 2

Temperature dependence of rate law

According to **equation 3** in the main text, the natural logarithm of the OER current and i/Q can be written as e**quation S4** and **S5**, respectively. Thus plotting the natural logarithm of the current or $\ln(i/Q)$ versus the inverse of the temperature at a given oxidative charge density would be linear, assuming a constant k_0.

$$ln(i) = ln(k_0) + ln(Q) + qQ/(TC_H\kappa_B) \qquad \textbf{(S4)}$$

$$\ln(i/Q) = ln(k_0) + qQ/(TC_H\kappa_B) \qquad \textbf{(S5)}$$

Supplementary Note 3

Linear versus Gaussian function

In literature[1], a linear function is used to describe the experimental data of the oxidative charge over potential. However, it fail to fit the half-bell like curve between Q and η (or E), but can be accurately well-fitted by Gaussian function (**equation 4** in the main text) as shown in **Figs. 1c-4c** in the main text. Gauss function

is an exponential-like function as shown in **Supplementary Fig. 16**. It would reduce to a linear function (**equation S6)** if $\left(\frac{E-w_3}{w_4}\right)^2 \to 0$ and $\left(\frac{E-w_3}{w_4}\right)^2 \ll 1$ for **equation 4** in the main text. This can explain why the linear function appears to be able to fit the experimental data of oxidative charge versus potential under a certain situations.

$$Q \approx w_1 + w_2[1 - \left(\frac{E-w_3}{w_4}\right)^2] \approx w_1 + w_2(1 + \frac{E-w_3}{w_4}) \qquad \textbf{(S6)}$$

Supplementary Note 4

Rate law in terms of current and external bias potential

Substituting **eq 4** into **eq 3** in the main text, we can get a new rate law written as **equation 5** in the main text and reproduced here (**equation S7**) for convenience, which describes the relationship between i and E (or η). Obviously, according to **equation S7** there will be *no* traditional Tafel equation. However, if the relationship between the oxidative charge and potential is approximately described by a linear function (**equation S6)** then **equation S7** can be reduced to **equation S8**. Thus the logarithm of **equation S8** can be written as **equation S9**. Under high overpotential (high oxidative charge density) where $AQ \gg \ln Q$, **equation S8 c**an be written as **equation S10** in a Tafel-like form, where $a = w_3 - \frac{2.3w_4}{Aw_2}[\log(k_0) + 0.434294\,A(w_1 + w_2)]$ and $b = \frac{2.3w_4}{Aw_2}$. This equation indicates that the applied potential is linearly proportional to the natural logarithm of the current, analogous to traditional Tafel polarization equation. This can explain why conventional Tafel equation appears to be able to fit the experimental potential versus log (current) under a certain situations. However, from **equation S10,**

it shows the so-called Tafel slope is determined by $\frac{2.3w_4}{Aw_2}$, which is related to A, w_2 and w_4 and is nothing to do with the reaction order for anodic process, while the Tafel intercept is given by $w_3 - \frac{2.3w_4}{Aw_2}[\log(k_0) + 0.434294\,A(w_1 + w_2)]$, which is related to $k_0, A\ and\ w_1 \sim w_4$ and is nothing to do with "exchange current density".

Under low overpotential (low oxidative charge density) where $AQ \ll \ln Q$, **equation S8 c**an be written as **equation S11**, where $a = w_3 - \frac{w_4}{w_2}(k_0 + w_1 + w_2)$ and $b = \frac{w_4}{w_2}$. This equation suggests that the current is linearly proportional to the applied, analogous to traditional linear polarization.

From these equations and their function graphs (Tafel plot), one or two straight lines can be obtained if the fitted data are selected partially as the authors[1] did, but it is absence of reliable theoretical basis. Tafel plot cannot by described by two intersection straight line (potential is bilinear in log(current)) in the plot of E versus $\log(i)$ as the authors[1] did, because some data cannot be on either of the lines (discontinue, see an example in **Fig. 1b** in the article[1], but can be explained by my rate throughout the potential range. In addition, the reaction order of OER from 1 to 3 (even zero) can be obtained if the fitted data are selected partially as the authors[1] did (likewise absence of theoretical basis).

$$i = k_0 \exp\left\{A\left\{\{w_1 + w_2 \exp\left[-\left(\frac{E-w_3}{w_4}\right)^2\right]\}\right\} * \left\{w_1 + w_2 \exp\left[-\left(\frac{E-w_3}{w_4}\right)^2\right]\right\} \quad \textbf{(S7)}$$

$$i = k_0 \exp\left\{A[w_1 + w_2(1 + \frac{E-w_3}{w_4})]\right\} * [w_1 + w_2(1 + \frac{E-w_3}{w_4})] \quad \textbf{(S8)}$$

$$\log(i) = \log(k_0) + 0.434294\,A[w_1 + w_2(1 + \frac{E-w_3}{w_4})] + \log([w_1 + w_2(1 + \frac{E-w_3}{w_4})]) \quad \textbf{(S9)}$$

$$E = w_3 - \frac{2.3w_4}{Aw_2}[\log(k_0) + 0.434294\,A(w_1 + w_2)] + \frac{2.3w_4}{Aw_2}\log(i) = a + b\log(i)$$

(S10)

$$E = w_3 - \frac{w_4}{w_2}(k_0 + w_1 + w_2) + \frac{w_4}{w_2}i = a + bi \quad \textbf{(S11)}$$

Supplementary Figures

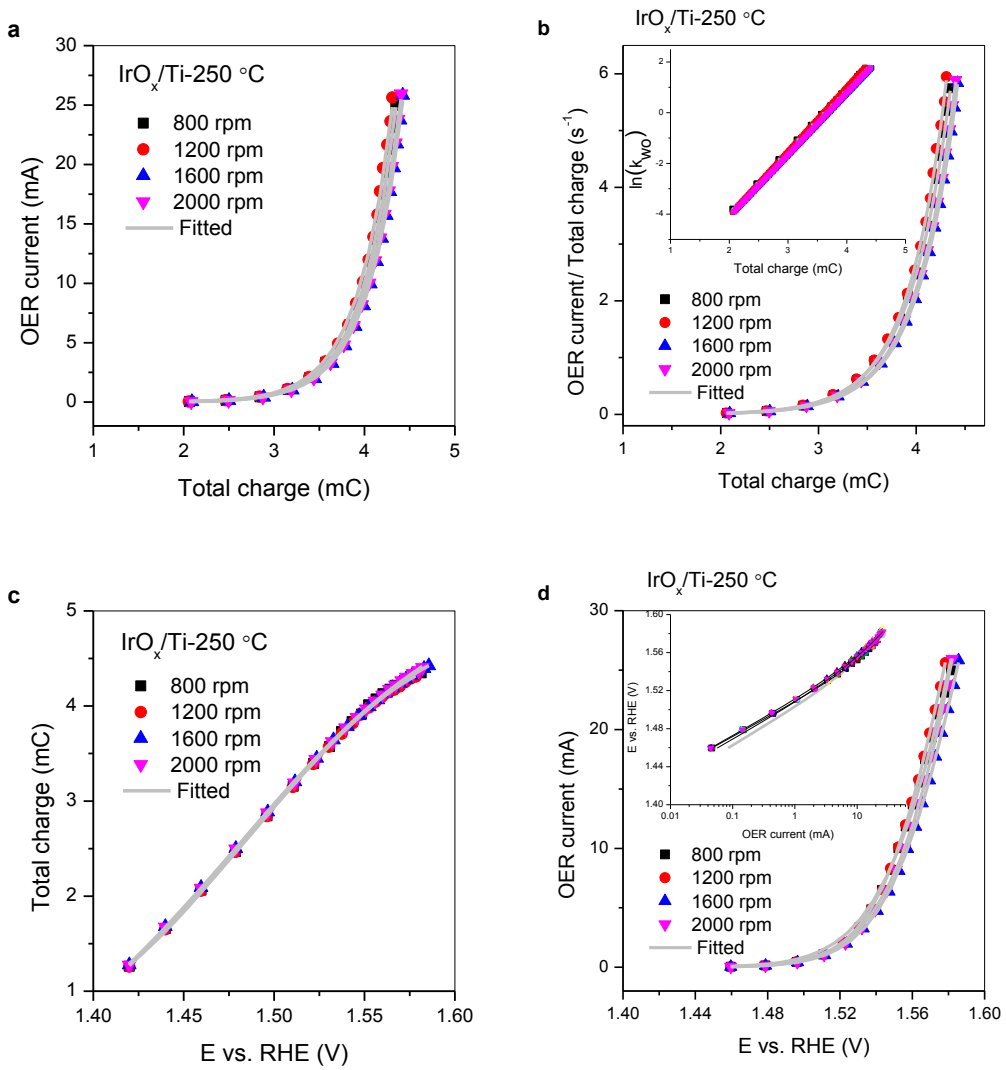

Supplementary Fig. 1 | Rotation speed dependent electrocatalytic response of IrO_x/Ti-250 ℃. a, OER current versus total charge (integral cathodic charge) from pulse voltammetry, the data were from the **Supplementary Fig. 18c** in the Article[1] and fitted by equation 3 in the main text (with results listed in **Table S7**). **b,** Corresponding relationship between $\text{OER current}/\text{Total charge}$ (or k_{wo}) and total charge with exponential fitting results listed in **Table S8. c,** Total charge (integral cathodic charge) vs. *i*R corrected potential from pulse voltammetry, the data were from **Supplementary Fig. 18b** in the Article[1] and fitted by **equation 4** in the main

text (with results listed in **Table S9). d,** OER current versus *i*R corrected potential, the data were from **Supplementary Fig. 18a** in the Article[1] and fitted by e**quation 5** in the main text (with results listed in **Table S10**), the insert shows Tafel plot (potential versus log(OER current) in milliamperes).

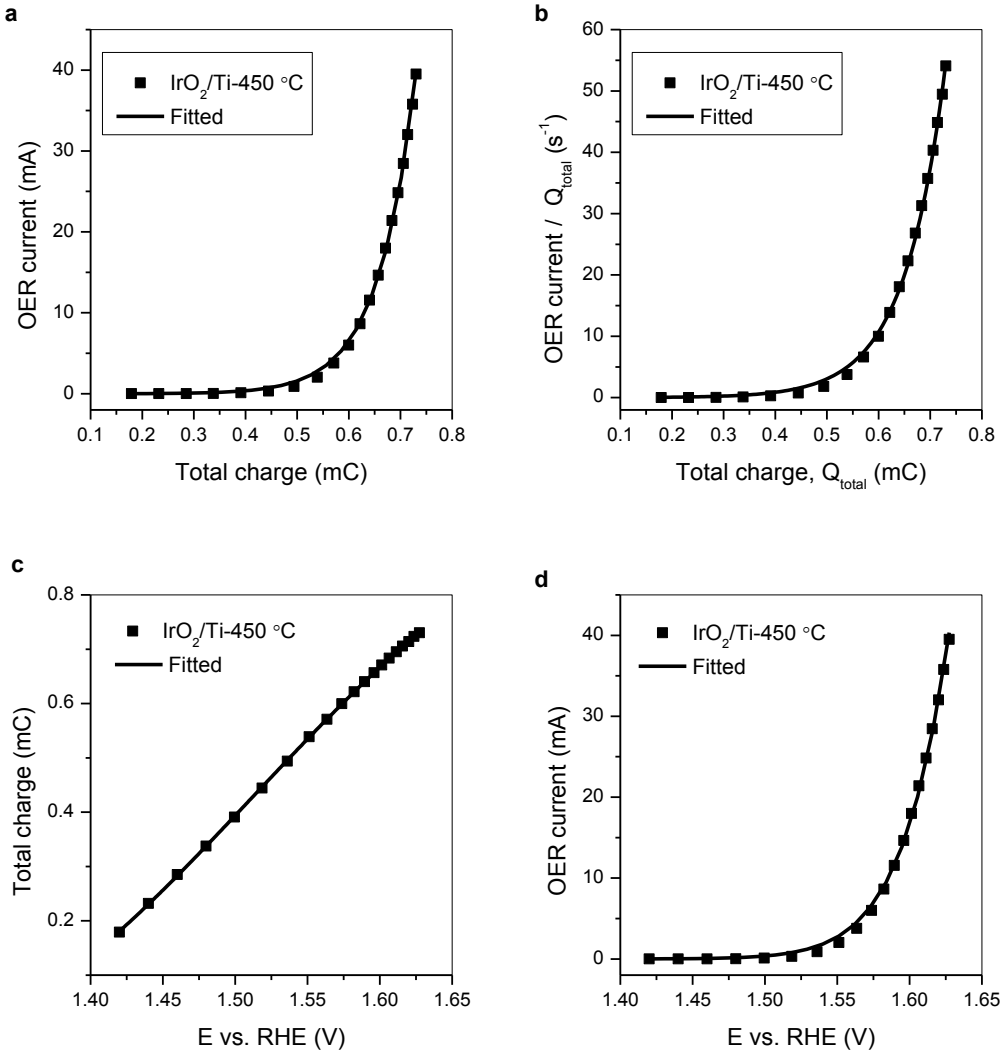

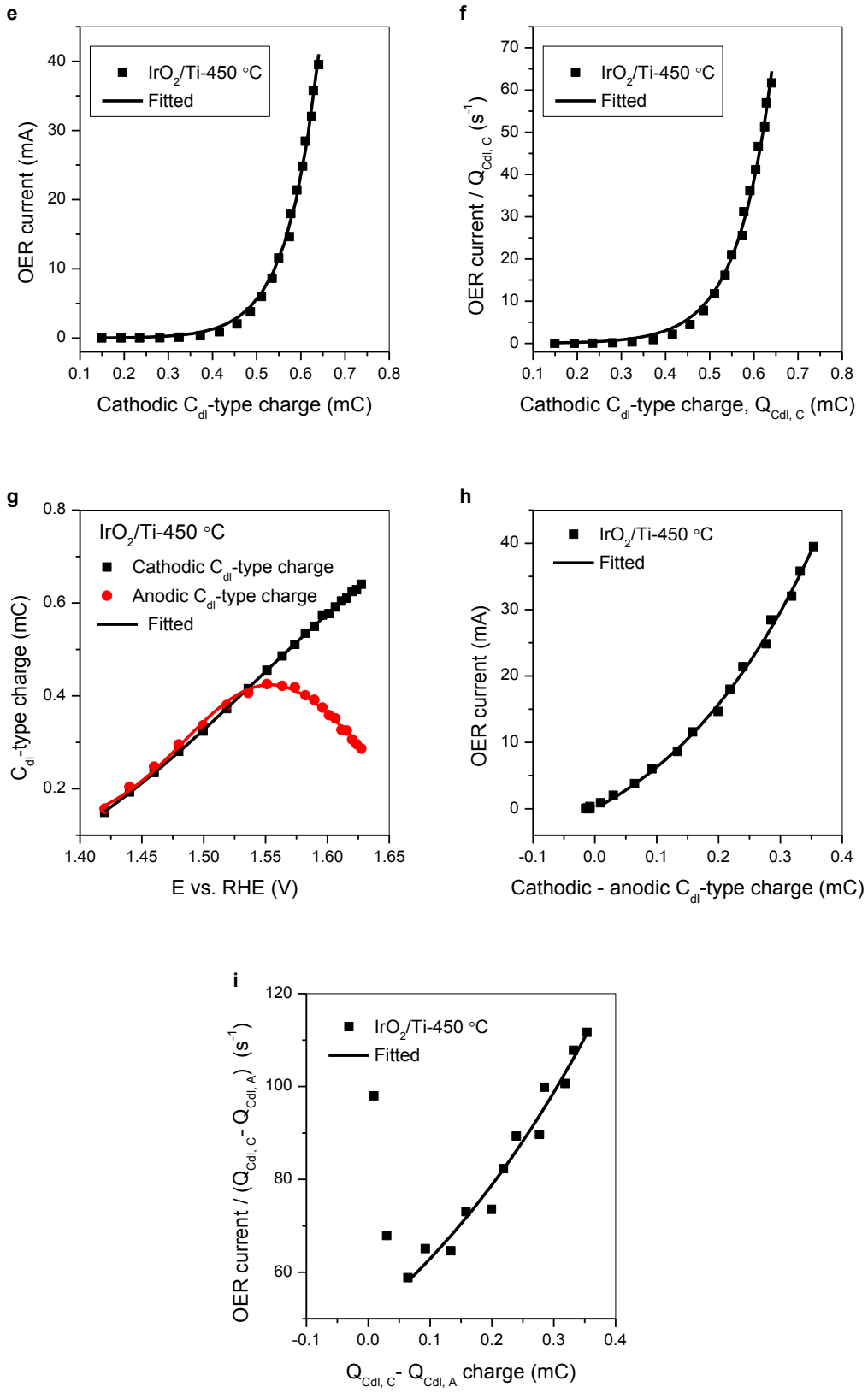

Supplementary Fig. 2 | Measured electrocatalytic response of IrO_x/Ti-450 ℃. a,

OER current versus total charge (integral cathodic charge) from pulse voltammetry, the data were from **Supplementary Fig. 2c** in the Article[1] and fitted by **equation 3** in the main text (with result $i = 6.1303 \times 10^{-3} \times \exp(12.3844 \times Q) \times Q$). **b,** Corresponding relationship between $\mathrm{OER\,current/Total\,charge}$ (or k_{wo}) and total charge with fitting result $k_{\mathrm{wo}} = 5.81{\times}10^{-2}{\times}\exp(12.52712{\times}Q)$, R^2 = 0.999. **c,** Total charge (integral cathodic charge) *vs*. *i*R corrected potential from pulse voltammetry, the data were from **Supplementary Fig. 2b** in the Article[1] and fitted by **equation 4** in the main text (with result $Q = 1.0979 - 1.1082{\times}\exp[-((\mathrm{x} - 1.2739)/0.33573)^2]$). **d,** OER current versus *i*R corrected potential, the data were from **Supplementary Fig. 2a** in the Article[1] and fitted by **equation 5** in the main text (with result $i = 8.063 \times 10^{-3} \times \exp[12.0594 \times Q(E)] \times Q(E)$, $Q(E)$ parameters see **Fig. c**). **e,** OER current versus cathodic C_{dl}-type charge, the data were from the **Supplementary Fig. 2d** in the Article[1] and fitted by **equation 3**. **f,** Corresponding relationship between $\mathrm{OER\,current/cathodic}\,C\mathrm{dl-type\,charge}$ (or k_{wo}) and cathodic C_{dl}-type charge, fitting with a single exponential function. **g,** C_{dl}-type charge vs. the iR corrected potential, the data were from **Supplementary Fig. 2f** in the Article[1] and fitted by **equation 4. h,** OER current versus the difference between cathodic and anodic C_{dl} -type charge, the data were from **Supplementary Fig. 2g** in the Article[1] and fitted by **equation 3**. **i,** Corresponding relationship between $\mathrm{OER\,current/the\,difference\,between\,cathodic\,and\,anodic}\,C\mathrm{dl-type\,charge}$ and the difference between cathodic and anodic C_{dl}-type charge, fitting with a single exponential function. Sample: fresh IrO_2/Ti-450 ℃.

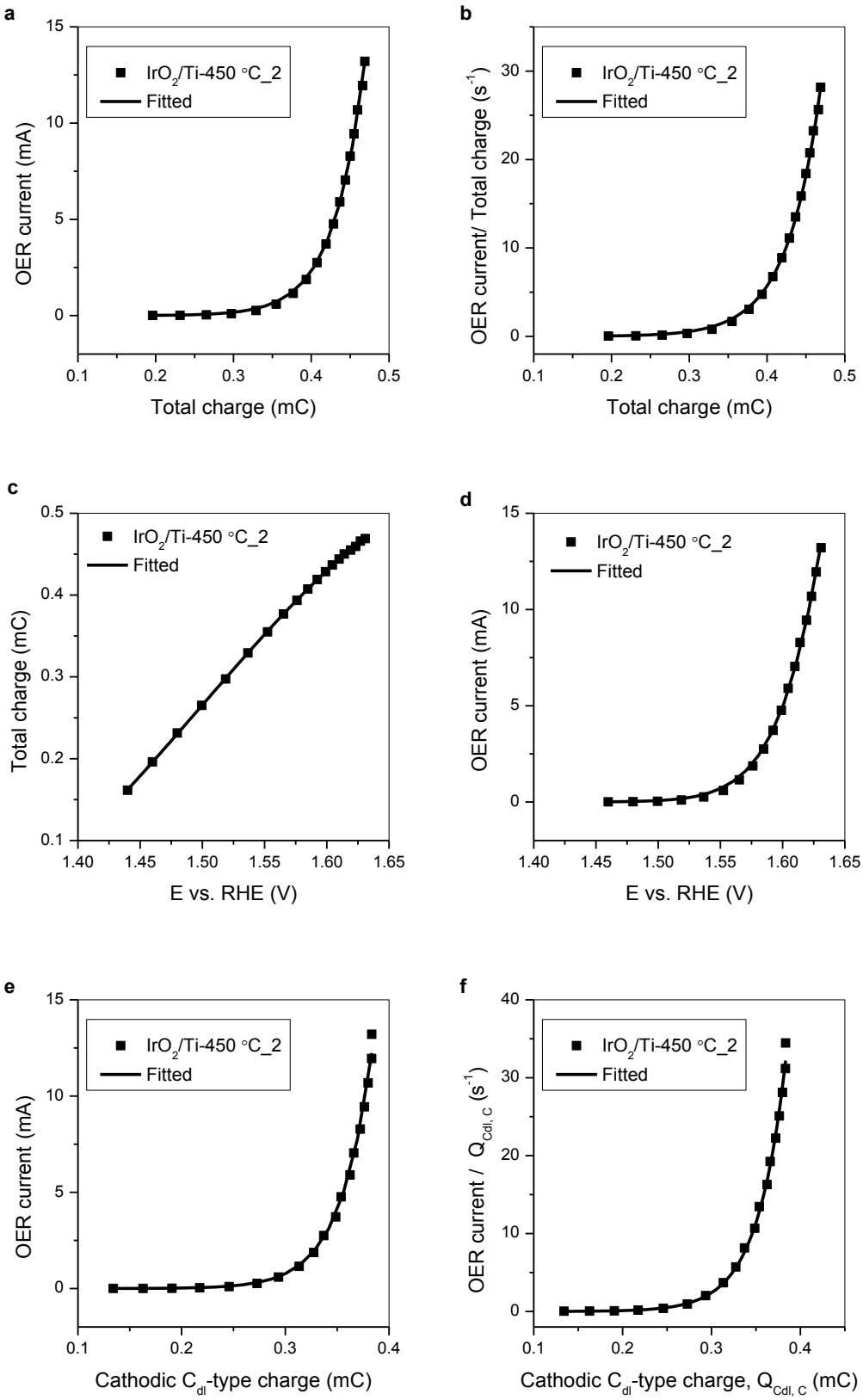
a
IrO2/Ti-450 °C_2
Fitted
OER current (mA)
Total charge (mC)
b
IrO2/Ti-450 °C_2
Fitted
OER current/ Total charge (s-1)
Total charge (mC)
c
IrO2/Ti-450 °C_2
Fitted
Total charge (mC)
E vs. RHE (V)
d
IrO2/Ti-450 °C_2
Fitted
OER current (mA)
E vs. RHE (V)
e
IrO2/Ti-450 °C_2
Fitted
OER current (mA)
Cathodic Cdl-type charge (mC)
f
IrO2/Ti-450 °C_2
Fitted
OER current / QCdl, C (s-1)
Cathodic Cdl-type charge, QCdl, C (mC)

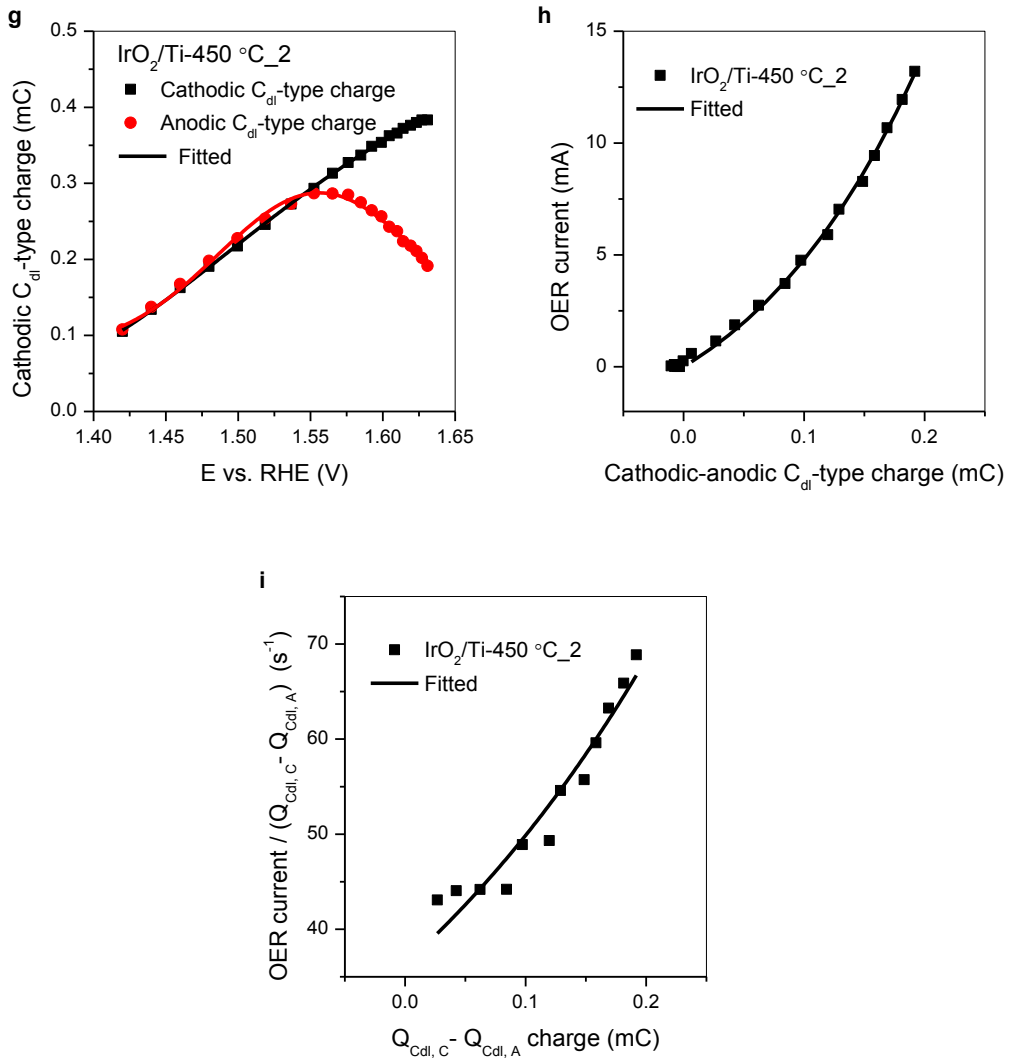

Supplementary Fig. 3 | Measured electrocatalytic response of used IrO_x/Ti-450 ℃. **a,** OER current versus total charge (integral cathodic charge) from pulse voltammetry, the data were from **Supplementary Fig. 3c** in the Article[1] and fitted by **equation 3 i**n the main text (with result $i = 5.61 \times 10^{-4} \times \exp(23.0818 \times Q) \times Q$). **b,** Corresponding relationship between $\text{OER current}/\text{Total charge}$ (or k_{wo}) and total charge with fitting result $k_{\text{wo}} = 5.32 * 10^{-4}\exp(23.19997 \times Q)$, R^2 = 0.999. **c,** Total charge (integral cathodic charge) vs. *i*R corrected potential from pulse voltammetry, the data were from **Supplementary Fig. 3b** in the Article[1] and fitted by **equation 4** in the main text (with result $Q = -0.1572 + 0.69363 \times \exp[-((x - 1.7386)/$

$0.33909)^2$]). **d,** OER current versus *i*R corrected potential, the data were from the **Supplementary Fig. 3a** in the Article[1] and fitted by **equation 5** in the main text (with result $i = 6.957 \times 10^{-4} \times \exp[22.606 \times Q(E)] \times Q(E)$, $Q(E)$ parameters see **Fig. c**). **e,** OER current versus cathodic C_{dl}-type charge, the data were from the **Supplementary Fig. 3d** in the Article[1] and fitted by **equation 3. f,** Corresponding relationship between $\text{OER current}/\text{cathodic } C\text{dl} - \text{type charge}$ (or k_{wo}) and cathodic C_{dl}-type charge, fitting with a single exponential function. g, C_{dl}-type charge vs. the *i*R corrected potential, the data were from **Supplementary Fig. 3f** in the Article[1] and fitted by **equation 4. h,** OER current versus the difference between cathodic and anodic C_{dl}-type charge, the data were from **Supplementary Fig. 3g** in the Article[1] and fitted by **equation 3. i,** Corresponding relationship between $\text{OER current}/\text{the difference between cathodic and anodic } C\text{dl} - \text{type charge}$ and the difference between cathodic and anodic C_{dl}-type charge, fitting with a single exponential function. Sample: partially deactivated IrO_2/Ti-450 ℃.

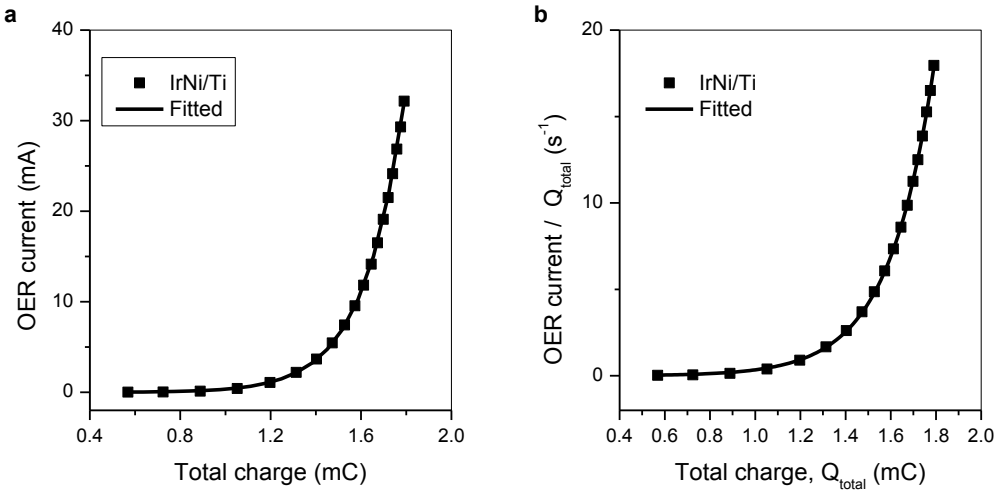

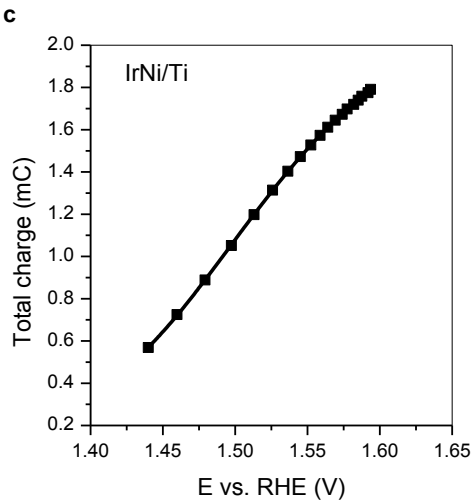
c
IrNi/Ti
Total charge (mC)
E vs. RHE (V)

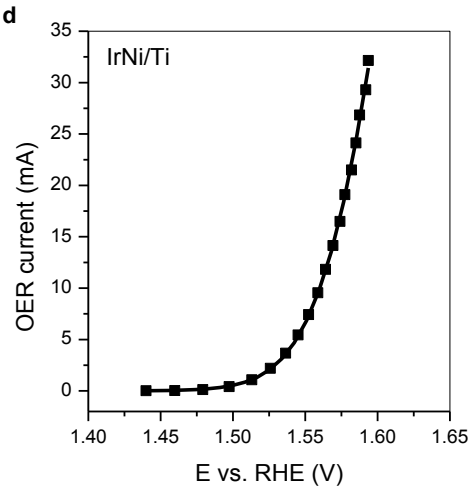
d
IrNi/Ti
OER current (mA)
E vs. RHE (V)

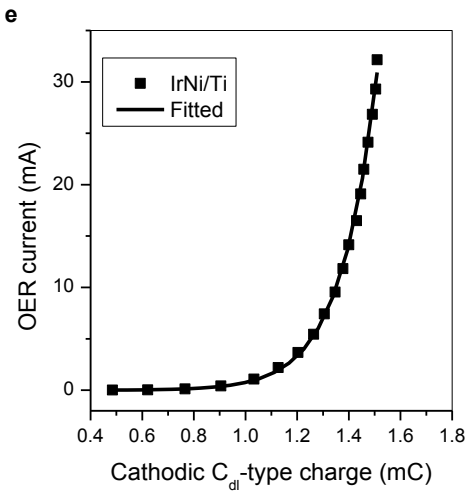
e
IrNi/Ti
Fitted
OER current (mA)
Cathodic C$_{dl}$-type charge (mC)

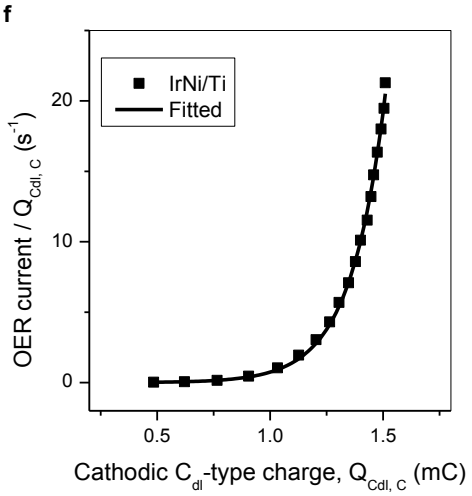
f
IrNi/Ti
Fitted
OER current / Q$_{Cdl, C}$ (s^{-1})
Cathodic C$_{dl}$-type charge, Q$_{Cdl, C}$ (mC)

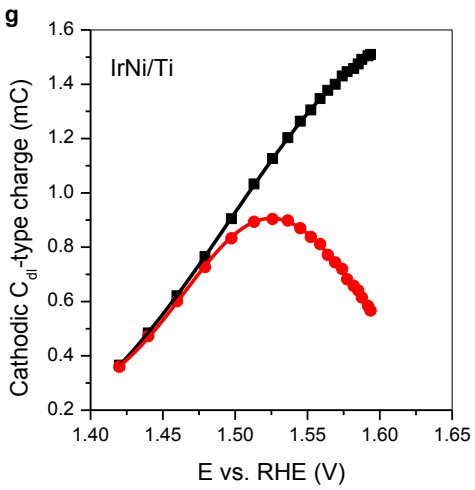
g
IrNi/Ti
Cathodic C$_{dl}$-type charge (mC)
E vs. RHE (V)

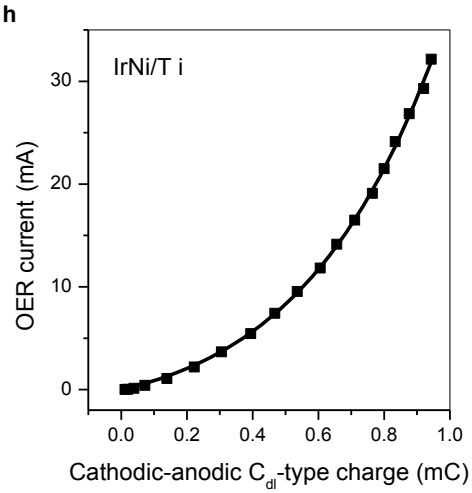
h
IrNi/T i
OER current (mA)
Cathodic-anodic C$_{dl}$-type charge (mC)

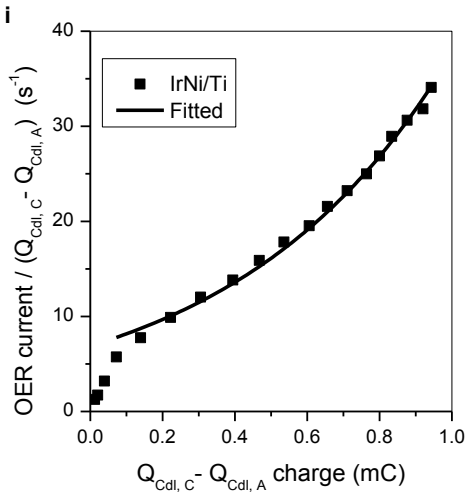

Supplementary Fig. 4 | Measured electrocatalytic response of IrNi/Ti. a, OER current versus total charge (integral cathodic charge) from pulse voltammetry, the data were from the **Supplementary Fig. 4c** in the Article[1] and fitted by **equation 3** in the main text (with result $i = 2.333 \times 10^{-3} \times \exp(4.99444 \times Q) \times Q$). **b,** Corresponding relationship between $\text{OER current}/\text{Total charge}$ (or $\boldsymbol{k_{wo}}$) and total charge with fitting result $k_{\text{wo}} = 2.35{\times}10^{-3}{\times}\exp(4.99134{\times}Q)$, R^2 = 0.9999. **c,** Total charge (integral cathodic charge) vs. *i*R corrected potential from pulse voltammetry, the data were from the **Supplementary Fig. 4b** in the Article[1] and fitted by **equation 4** in the main text (with result $Q = 2.1049 - 1.7491 \times \exp[-((\text{x} - 1.381)/0.16279)^2]$). **d,** OER current versus *i*R corrected potential, the data were from **Supplementary Fig. 4a** in the Article[1] and fitted by **equation 5** in the main text (with result $i = 2.2 \times 10^{-3} \times \exp[5.02834{\times}\, Q(E)] \times Q(E)$, $Q(E)$ parameters see **Fig. c**). **e,** OER current versus cathodic C_{dl}-type charge, the data were from **Supplementary Fig. 4d** in the Article[1] and fitted b**y equation 3. f,** Corresponding relationship between $\text{OER current}/\text{cathodic } C\text{dl} - \text{type charge}$ (or $\boldsymbol{k_{wo}}$) and cathodic C_{dl}-type charge, fitting with a single exponential function. **g,** C_{dl}-type charge vs. the *i*R corrected potential, the data were from the **Supplementary Fig. 4f** in the Article[1] and fitted by

equation 4. h, OER current versus the difference between cathodic and anodic C_{dl}-type charge, the data were from **Supplementary Fig. 4g** in the Article[1] and fitted by **equation 3. i,** Corresponding relationship between OER current/the difference between cathodic and anodic Cdl − type charge and the difference between cathodic and anodic C_{dl}-type charge, fitting with a single exponential function. Sample: IrNi/Ti.

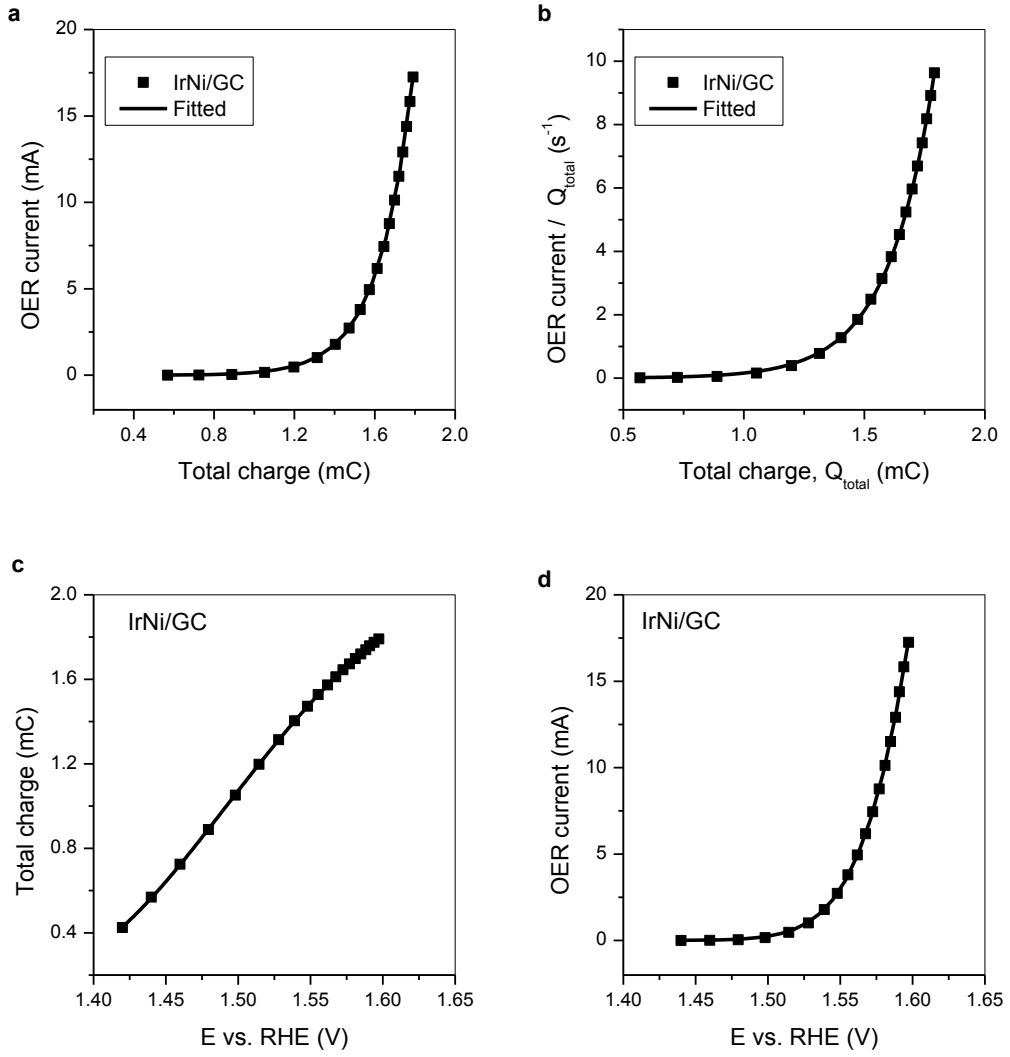

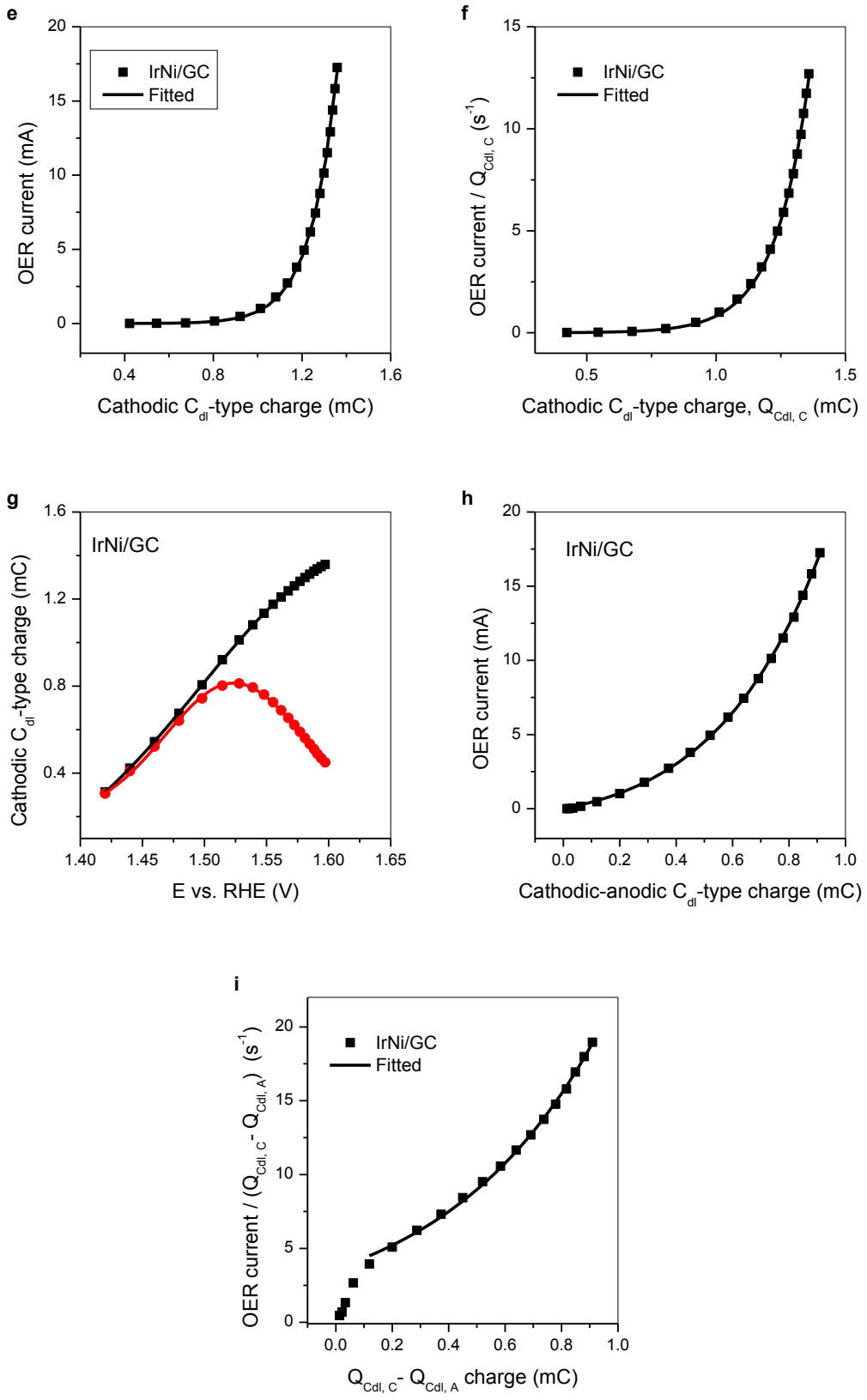
e
IrNi/GC
Fitted
OER current (mA)
Cathodic C_{dl}-type charge (mC)
f
IrNi/GC
Fitted
OER current / $Q_{Cdl, C}$ (s^{-1})
Cathodic C_{dl}-type charge, $Q_{Cdl, C}$ (mC)
g
IrNi/GC
Cathodic C_{dl}-type charge (mC)
E vs. RHE (V)
h
IrNi/GC
OER current (mA)
Cathodic-anodic C_{dl}-type charge (mC)
i
IrNi/GC
Fitted
OER current / ($Q_{Cdl, C}$ - $Q_{Cdl, A}$) (s^{-1})
$Q_{Cdl, C}$ - $Q_{Cdl, A}$ charge (mC)

Supplementary Fig. 5 | Measured electrocatalytic response of IrNi/GC. a, OER current versus total charge (integral cathodic charge) from pulse voltammetry, the data were from **Supplementary Fig. 5c** in the Article[1] and fitted by **equation 3** in the main text (with result $i = 8.948 \times 10^{-4} \times \exp(5.18545 \times Q) \times Q$). **b,** Corresponding relationship between $\mathrm{OER\,current/Total\,charge}$ (or k_{wo}) and total charge with fitting result $k_{\mathrm{wo}} = 8.824{\times}10^{-4}{\times}\exp(5.19351{\times}Q)$, R^2 = 0.9999. **c**, Total charge (integral cathodic charge) vs. *i*R corrected potential from pulse voltammetry, the data were from **Supplementary Fig. 5b** in the Article[1] and fitted by **equation 4** in the main text (with result $Q = 2.2016 - 1.9852 \times \exp[-((\mathrm{x} - 1.3553)/0.19259)^2]$). **d**, OER current versus iR corrected potential, the data were from **Supplementary Fig. 5a** in the Article[1] and fitted by **equation 5** in the main text (with result $i = 9.152 \times 10^{-4} \times \exp[5.17114{\times}\, Q(E)] \times Q(E)$, $\boldsymbol{Q(E)}$ parameters see **Fig. c**). **e**, OER current versus cathodic C_{dl}-type charge, the data were from **Supplementary Fig. 5d** in the Article[1] and fitted by **equation 3**. **f**, Corresponding relationship between $\mathrm{OER\,current/cathodic\,Cdl-type\,charge}$ (or k_{wo}) and cathodic C_{dl}-type charge, fitting with a single exponential function. **g**, C_{dl}-type charge vs. the *i*R corrected potential, the data were from **Supplementary Fig. 5f** in the Article[1] and fitted by **equation 4**. **h**, OER current versus the difference between cathodic and anodic C_{dl}-type charge, the data were from **Supplementary Fig. 5g** in the Article[1] and fitted by **equation 2**. **i**, Corresponding relationship between $\mathrm{OER\,current/the\,difference\,between\,cathodic\,and\,anodic\,Cdl-type\,charge}$ and the difference between cathodic and anodic C_{dl}-type charge, fitting with a single exponential function. Sample: IrNi/GC (GC: glassy carbon).

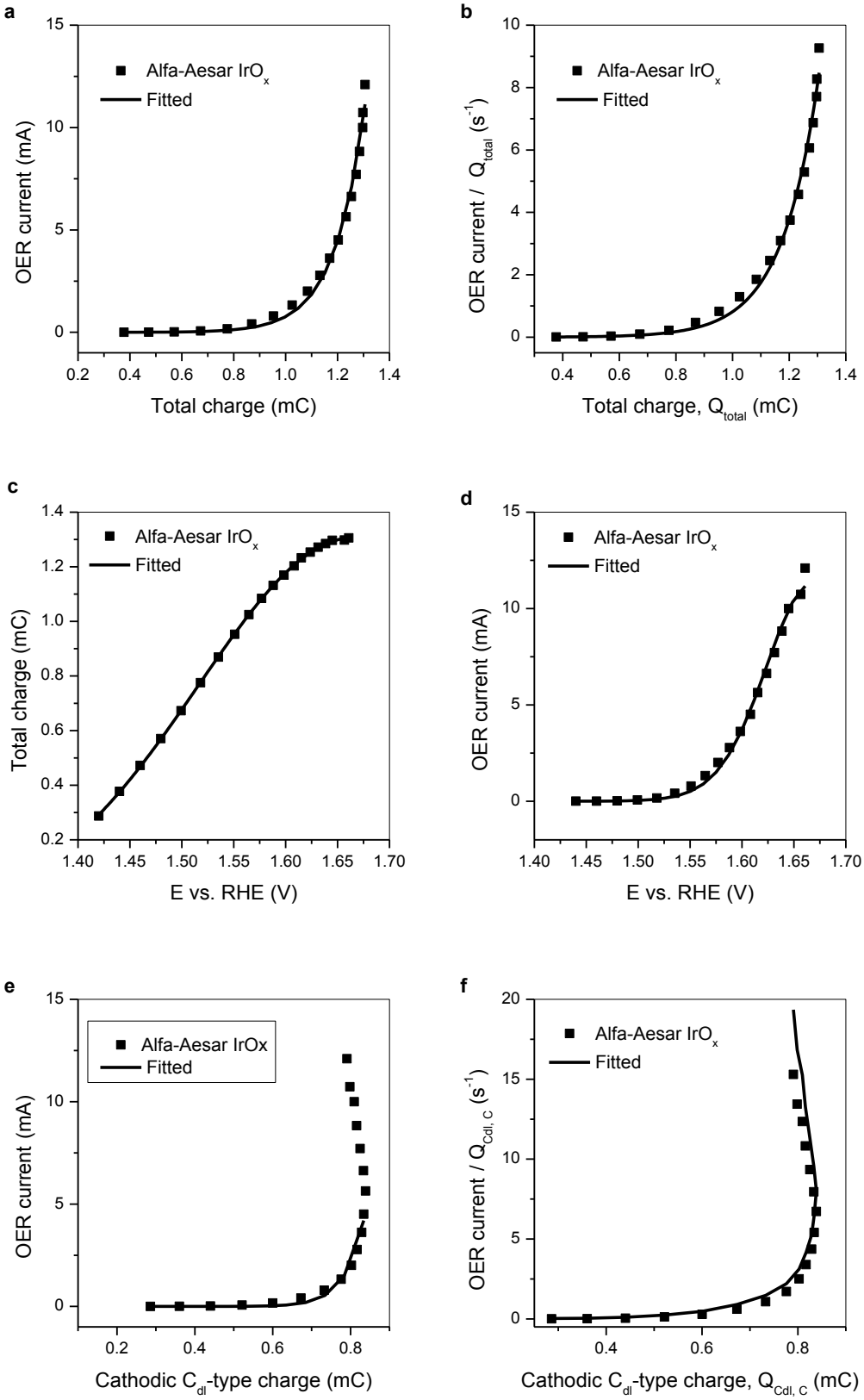
a
OER current (mA)
Total charge (mC)
Alfa-Aesar IrO$_x$
Fitted
b
OER current / Q_{total} (s^{-1})
Total charge, Q_{total} (mC)
Alfa-Aesar IrO$_x$
Fitted
c
Total charge (mC)
E vs. RHE (V)
Alfa-Aesar IrO$_x$
Fitted
d
OER current (mA)
E vs. RHE (V)
Alfa-Aesar IrO$_x$
Fitted
e
OER current (mA)
Cathodic C_{dl}-type charge (mC)
Alfa-Aesar IrOx
Fitted
f
OER current / $Q_{Cdl, C}$ (s^{-1})
Cathodic C_{dl}-type charge, $Q_{Cdl, C}$ (mC)
Alfa-Aesar IrO$_x$
Fitted

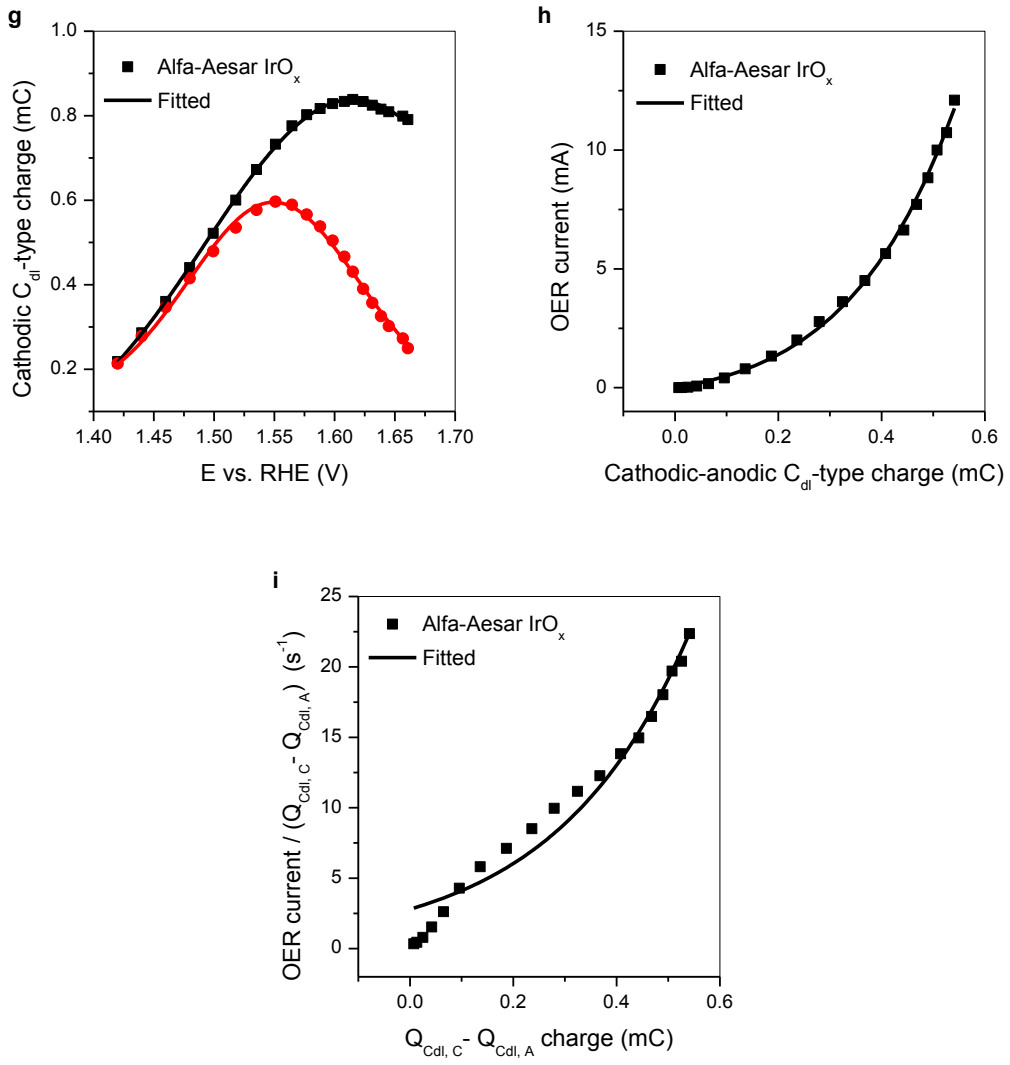

Supplementary Fig. 6 | Measured electrocatalytic response of Alfa-Aesar IrO_x. a, OER current versus total charge (integral cathodic charge) from pulse voltammetry, the data were from **Supplementary Fig. 6c** in the Article[1] and fitted by **equation 3** in the main text (with result $i = 2.881 \times 10^{-4} \times \exp(7.88418 \times Q) \times Q$). **b**, Corresponding relationship between $\text{OER current}/\text{Total charge}$ (or k_{wo}) and total charge with fitting result $\text{k}_{\text{wo}} = 3.861{\times}10^{-4}{\times}\exp(7.65494{\times}\text{Q})$, R^2 = 0.99. **c**, Total charge (integral cathodic charge) vs. *i*R corrected potential from pulse voltammetry, the data were from **Supplementary Fig. 6b** in the Article[1] and fitted by **equation 4** in the main text (with result $Q = -0.0709 + 1.3784 \times \exp[-((\text{x} - 1.6671)/$

$0.21377)^2$]). **d**, OER current versus iR corrected potential, the data were from **Supplementary Fig. 6a** in the Article[1] and fitted by **equation 5** in the main text (with result $i = 3.26 \times 10^{-4} \times \exp[7.78851 \times Q(E)] \times Q(E)$, $Q(E)$ parameters see **Fig. c**). **e**, OER current versus cathodic C_{dl}-type charge, the data were from **Supplementary Fig. 6d** in the Article[1] and fitted by **equation 3**. **f**, Corresponding relationship between OER current/cathodic Cdl − type charge (or k_{wo}) and cathodic C_{dl}-type charge, fitting with a single exponential function. **g**, C_{dl}-type charge vs. the *i*R corrected potential, the data were from **Supplementary Fig. 6f** in the Article[1] and fitted by **equation 4**. **h**, OER current versus the difference between cathodic and anodic C_{dl}-type charge, the data were from **Supplementary Fig. 6g** in the Article[1] and fitted by **equation 3**. **i**, Corresponding relationship between OER current/the difference between cathodic and anodic Cdl − type charge and the difference between cathodic and anodic C_{dl}-type charge, fitting with a single exponential function. Sample: commercial Alfa-Aesar IrO_x powder.

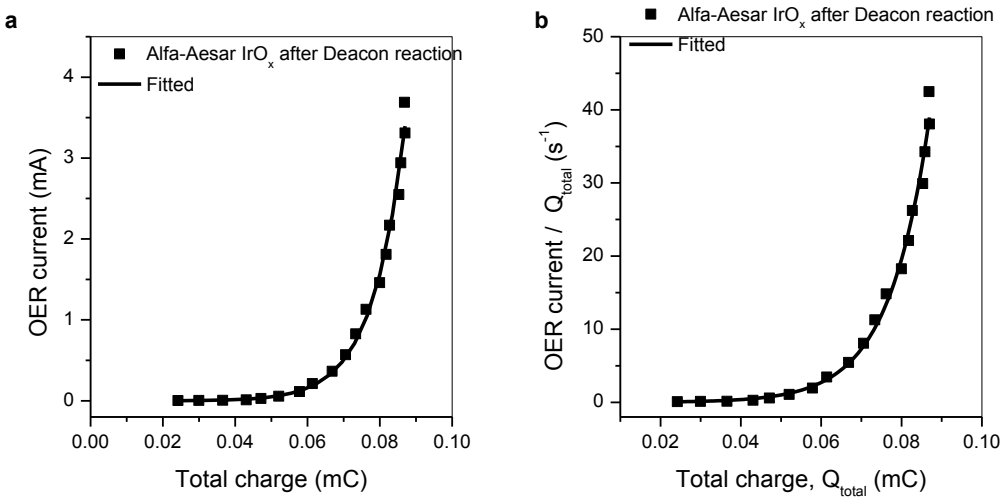

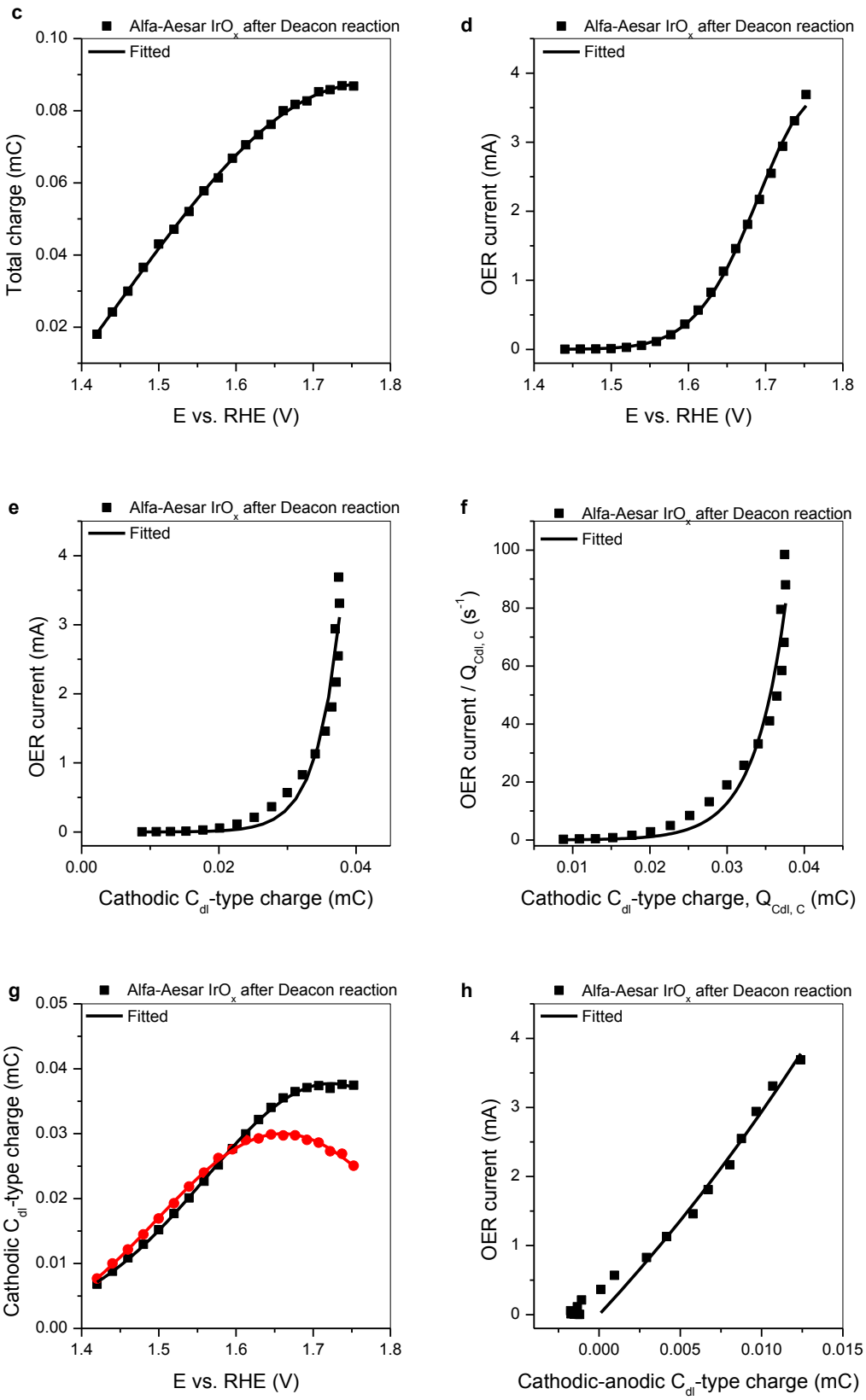
c
Alfa-Aesar IrO$_x$ after Deacon reaction
Fitted
Total charge (mC)
E vs. RHE (V)
d
Alfa-Aesar IrO$_x$ after Deacon reaction
Fitted
OER current (mA)
E vs. RHE (V)
e
Alfa-Aesar IrO$_x$ after Deacon reaction
Fitted
OER current (mA)
Cathodic C$_{dl}$-type charge (mC)
f
Alfa-Aesar IrO$_x$ after Deacon reaction
Fitted
OER current / Q$_{Cdl, C}$ (s^{-1})
Cathodic C$_{dl}$-type charge, Q$_{Cdl, C}$ (mC)
g
Alfa-Aesar IrO$_x$ after Deacon reaction
Fitted
Cathodic C$_{dl}$-type charge (mC)
E vs. RHE (V)
h
Alfa-Aesar IrO$_x$ after Deacon reaction
Fitted
OER current (mA)
Cathodic-anodic C$_{dl}$-type charge (mC)

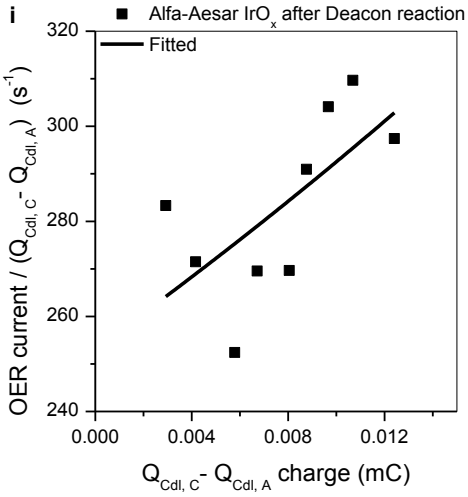

Supplementary Fig. 7 | Measured electrocatalytic response of Alfa-Aesar IrO_x post-Deacon. a, OER current versus total charge (integral cathodic charge) from pulse voltammetry, the data were from **Supplementary Fig. 7c** in the Article[1] and fitted by **equation 3** in the main text (with result $i = 6.723 \times 10^{-3} \times \exp(99.6518 \times Q) \times Q$). **b**, Corresponding relationship between OER current/Total charge (or $\boldsymbol{k_{wo}}$) and total charge with fitting result $k_{wo} = 7.29 \times 10^{-3} \times \exp(98.69792 \times Q)$, R^2 = 0.991. **c**, Total charge (integral cathodic charge) vs. *i*R corrected potential from pulse voltammetry, the data were from **Supplementary Fig. 7b** in the Article[1] and fitted by **equation 4** in the main text (with result $Q = -0.0723 + 0.15982 \times \exp[-((x - 1.7687)/0.46304)^2]$). **d**, OER current versus *i*R corrected potential, the data were from **Supplementary Fig. 7a** in the Article[1] and fitted by **equation 5** in the main text (with result $i = 7.501 \times 10^{-3} \times \exp[98.3939 \times Q(E)] \times Q(E)$, $Q(E)$ parameters see **Fig. c**). **e**, OER current versus cathodic C_{dl}-type charge, the data were from **Supplementary Fig. 7d in** the Article[1] and fitted by **equation 3**. **f**, Corresponding relationship between OER current/cathodic Cdl − type charge (or $\boldsymbol{k_{wo}}$) and cathodic C_{dl}-type charge, fitting with a single exponential function. **g**, C_{dl}-type charge vs. the *i*R corrected

potential, the data were from **Supplementary Fig. 7f** in the Article[1] and fitted by **equation 4**. **h**, OER current versus the difference between cathodic and anodic C_{dl}-type charge, the data were from **Supplementary Fig. 7g** in the Article[1] and fitted **by equation 3**. **i**, Corresponding relationship between OER current/the difference between cathodic and anodic Cdl − type charge and the difference between cathodic and anodic C_{dl}-type charge, fitting with a single exponential function. Sample: commercial Alfa-Aesar IrO_x powder after treatment in the Deacon reaction.

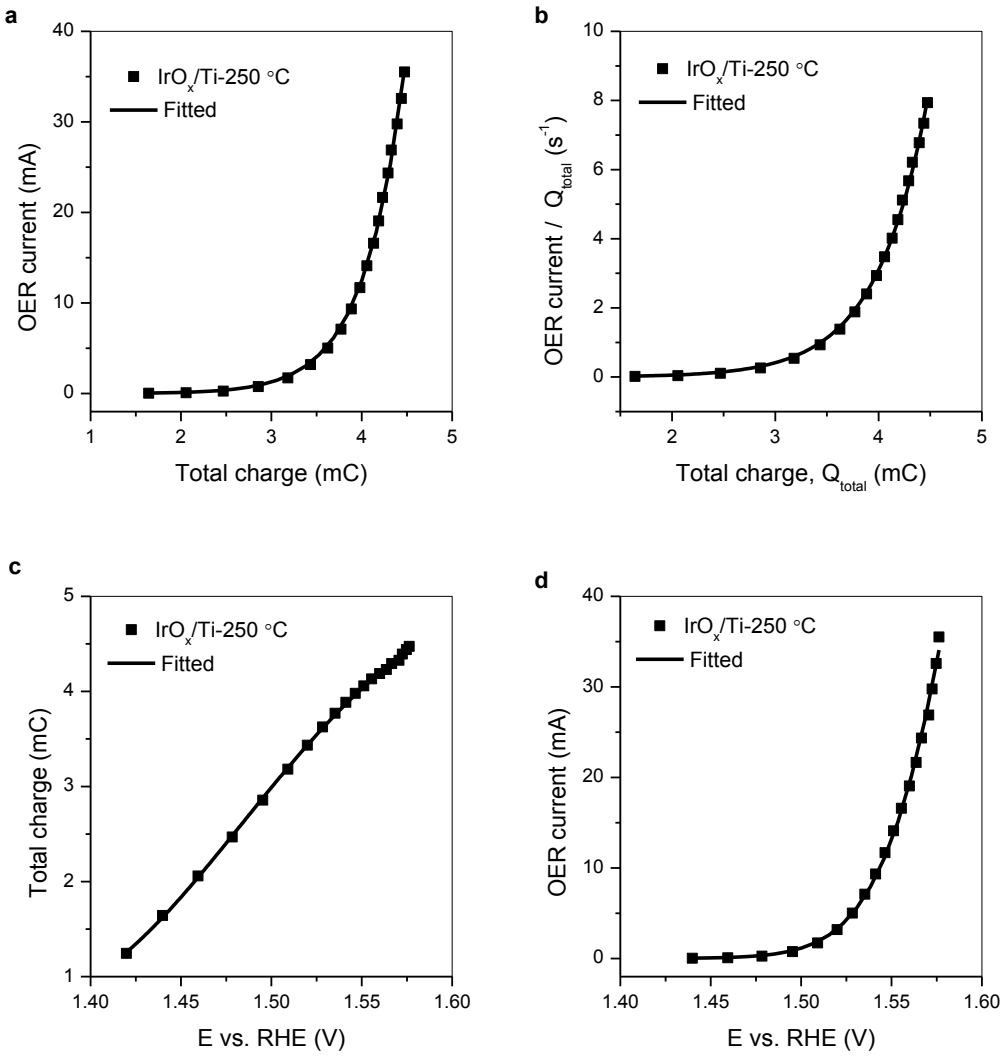

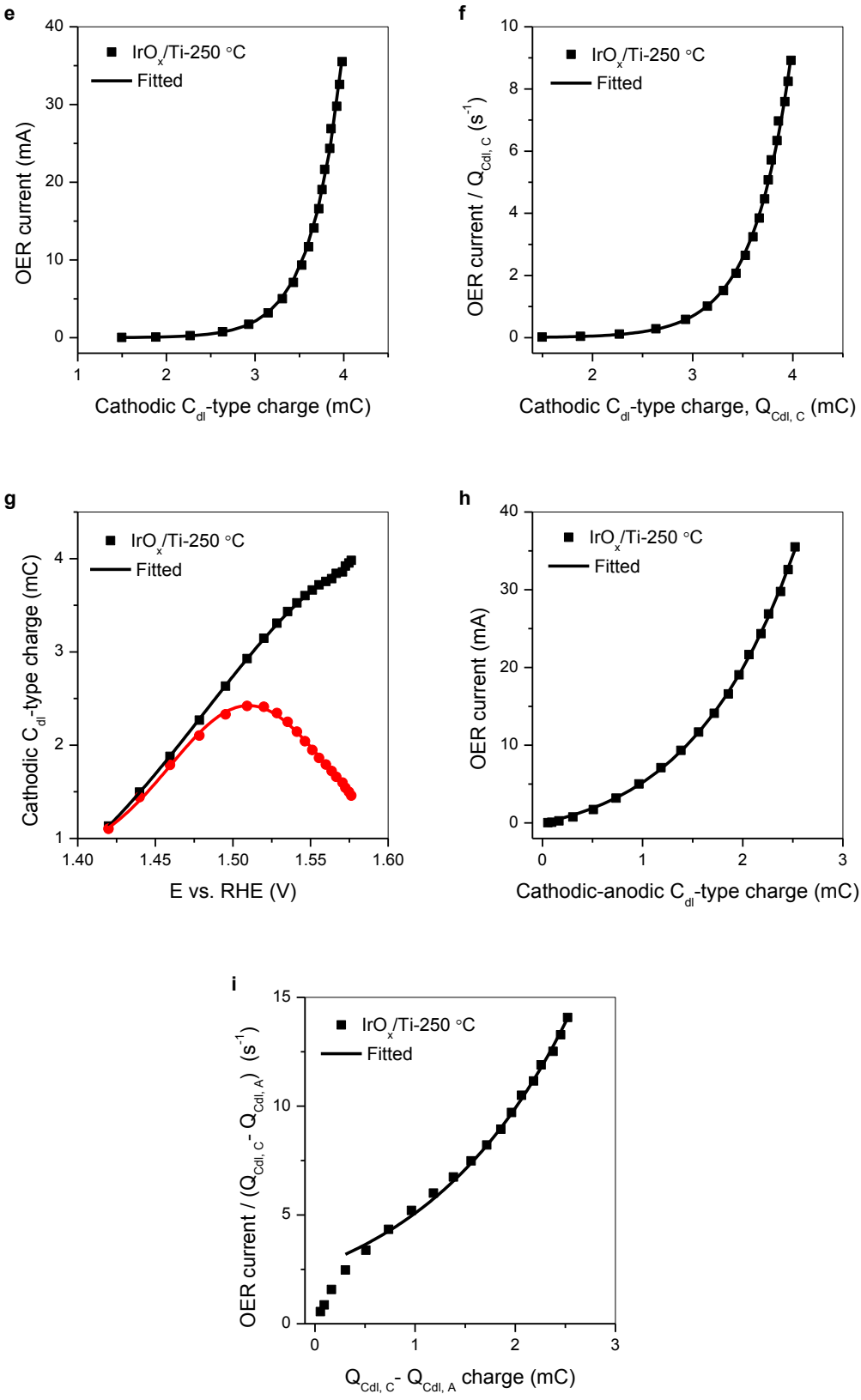
e
IrOx/Ti-250 °C
Fitted
OER current (mA)
Cathodic Cdl-type charge (mC)
f
IrOx/Ti-250 °C
Fitted
OER current / QCdl, C (s-1)
Cathodic Cdl-type charge, QCdl, C (mC)
g
IrOx/Ti-250 °C
Fitted
Cathodic Cdl-type charge (mC)
E vs. RHE (V)
h
IrOx/Ti-250 °C
Fitted
OER current (mA)
Cathodic-anodic Cdl-type charge (mC)
i
IrOx/Ti-250 °C
Fitted
OER current / (QCdl, C - QCdl, A) (s-1)
QCdl, C - QCdl, A charge (mC)

Supplementary Fig. 8 | Measured electrocatalytic response of IrO_x/Ti-250° C. a, OER current versus total charge (integral cathodic charge) from pulse voltammetry, the data were from **Supplementary Fig. 8c** in the Article[1] and fitted by **equation 3** in the main text (with result $i = 1.053 \times 10^{-3} \times \exp(1.99789 \times Q) \times Q$). **b**, Corresponding relationship between $\mathrm{OER\ current/Total\ charge}$ (or k_{wo}) and total charge with fitting result $k_{\mathrm{wo}} = 9.89 \times 10^{-4} \times \exp(2.01241 \times Q)$, R^2 = 0.999. **c**, Total charge (integral cathodic charge) vs. *i*R corrected potential from pulse voltammetry, the data were from **Supplementary Fig. 8b** in the Article[1] and fitted by **equation 4** in the main text (with result $Q = 5.3635 - 4.5744 \times \exp[-((\mathrm{x} - 1.3651)/0.16654)^2]$). **d**, OER current versus *i*R corrected potential, the data were from **Supplementary Fig. 8a** in the Article[1] and fitted by **equation 5** in the main text (with result $i = 8.09 \times 10^{-4} \times \exp[2.05871 \times Q(E)] \times Q(E)$, $Q(E)$ parameters see **Fig. c**). **e**, OER current versus cathodic C_{dl}-type charge, the data were from **Supplementary Fig. 8d** in the Article[1] and fitted by **equation 3**. **f**, Corresponding relationship between $\mathrm{OER\ current/cathodic\ Cdl-type\ charge}$ (or k_{wo}) and cathodic C_{dl}-type charge, fitting with a single exponential function. **g**, C_{dl}-type charge vs. the *i*R corrected potential, the data were from **Supplementary Fig. 8f** in the Article[1] and fitted by **equation 4**. **h**, OER current versus the difference between cathodic and anodic C_{dl}-type charge, the data were from **Supplementary Fig. 8g** in the Article[1] and fitted by **equation 3**. **i**, Corresponding relationship between $\mathrm{OER\ current/the\ difference\ between\ cathodic\ and\ anodic}\ C\mathrm{dl-type\ charge}$ and the difference between cathodic and anodic C_{dl}-type charge, fitting with a single exponential function. Sample: IrO_x/Ti-250 ℃.

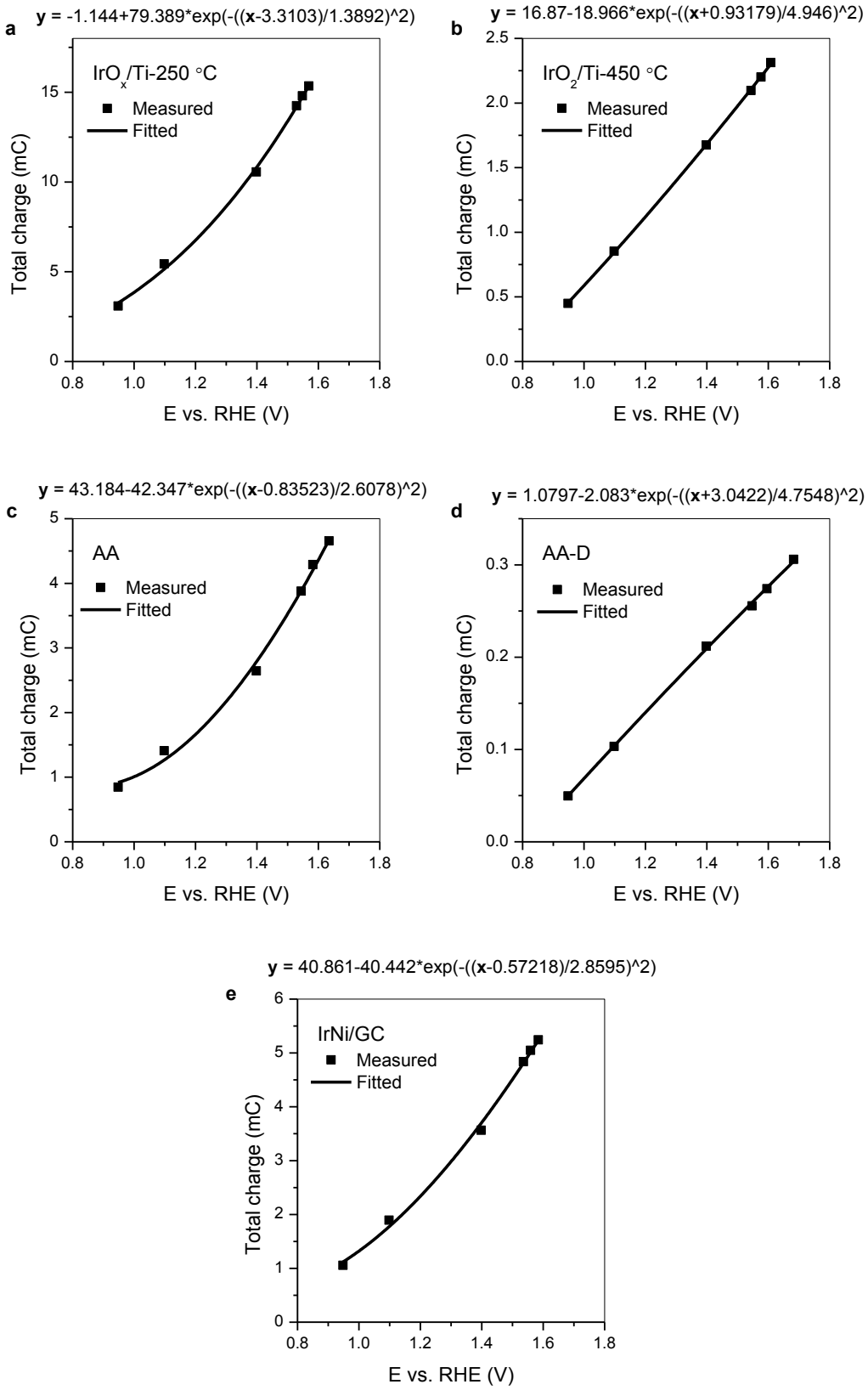
a
y = -1.144+79.389*exp(-((x-3.3103)/1.3892)^2)
IrOx/Ti-250 °C
Measured
Fitted
Total charge (mC)
E vs. RHE (V)
b
y = 16.87-18.966*exp(-((x+0.93179)/4.946)^2)
IrO2/Ti-450 °C
Measured
Fitted
Total charge (mC)
E vs. RHE (V)
c
y = 43.184-42.347*exp(-((x-0.83523)/2.6078)^2)
AA
Measured
Fitted
Total charge (mC)
E vs. RHE (V)
d
y = 1.0797-2.083*exp(-((x+3.0422)/4.7548)^2)
AA-D
Measured
Fitted
Total charge (mC)
E vs. RHE (V)
e
y = 40.861-40.442*exp(-((x-0.57218)/2.8595)^2)
IrNi/GC
Measured
Fitted
Total charge (mC)
E vs. RHE (V)

Supplementary Fig. 9 | Total charge of selected samples. Charge determined by integral pulse voltammetry analysis in the broad potential window. Protocol: cathodic potential: 0.75 V, anodic potentials: 0.95 V to 1.7 V non-*i*R corrected potentials. The figure plots the *i*R corrected potentials. The data were from **Supplementary Fig. 10** in the Article[1] and fitted by **equation 4** in the main text with fitting result as marked.

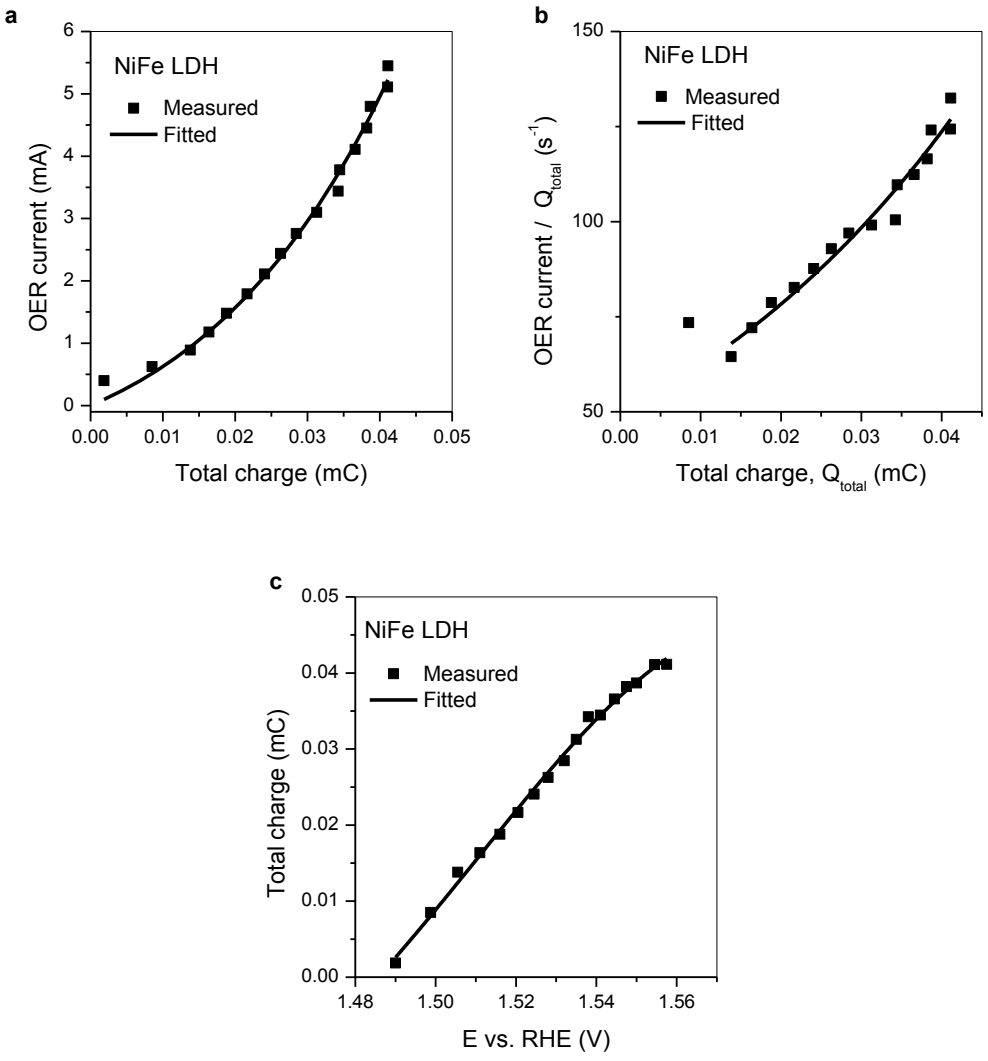

Supplementary Fig. 10 | Electrochemical response of NiFe LDH. a, OER current versus total charge (integral cathodic charge) from pulse voltammetry, the data were from **Supplementary Fig. 17a** in the Article[1] and fitted by **equation 3** in the main text (with result $i = 49.677 \times \exp(22.823 \times Q) \times Q$). **b**, Corresponding relationship

between OER current/Total charge (or k_{wo}) and total charge with fitting result $k_{wo} = 49.57177 \times \exp(22.86216 \times Q)$, R^2 = 0.969. **c**, Total charge (integral cathodic charge) vs. *i*R corrected potential from pulse voltammetry, the data were from **Supplementary Fig. 17b** in the Article[1] and fitted by **equation 4** in the main text (with result $Q = -0.03192 + 0.078654 \times \exp[-((x - 1.5835)/0.10298)^2]$). Sample: NiFe layered double hydroxide.

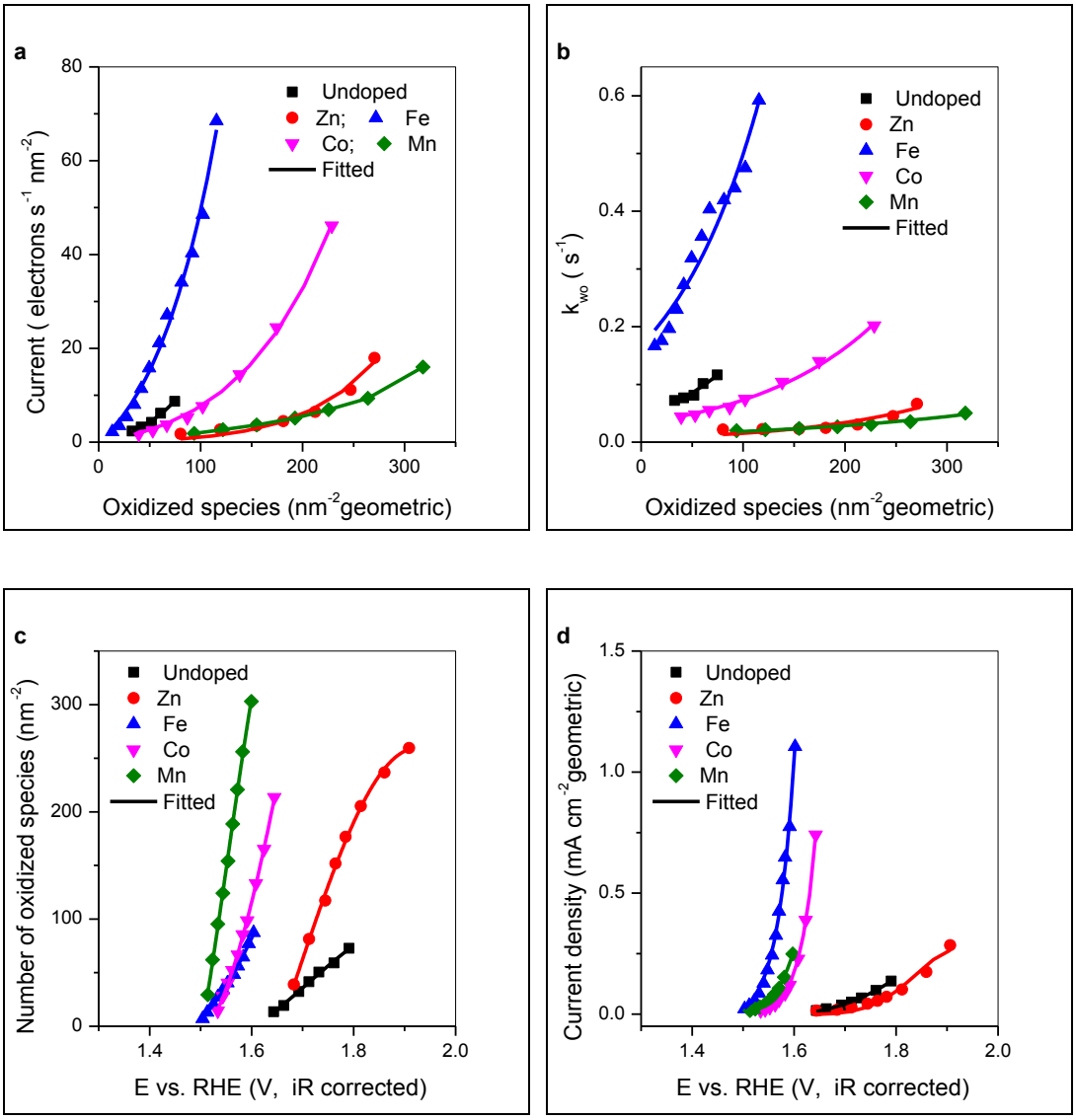

Supplementary Fig. 11 | Measured electrocatalytic response of doped nickel oxides. a, OER current density versus the density of oxidized species from

spectroelectrochemistry, the data were from **Fig. 3c** in the Article[2] and fitted by **equation 3** in the main text (with result listed in **Table S11**). **b**, Corresponding relationship between $\text{OER current}/\text{Total charge}$ (or k_{wo}) and total charge with fitting result with result listed in **Table S12**). **c**, Total charge (integral cathodic charge) *vs*. *i*R corrected potential from pulse voltammetry, the data were from **Supplementary Fig. 8b** in the Article[2] and fitted by **equation 4** in the main text (with result listed in **Table S13**). **d**, OER current versus *i*R corrected potential, the data were from **Supplementary Fig. 8a** in the Article[2] and fitted by **equation 5** in the main text (with result in **Table S14**, $Q(E)$ parameters see **Fig. c**).

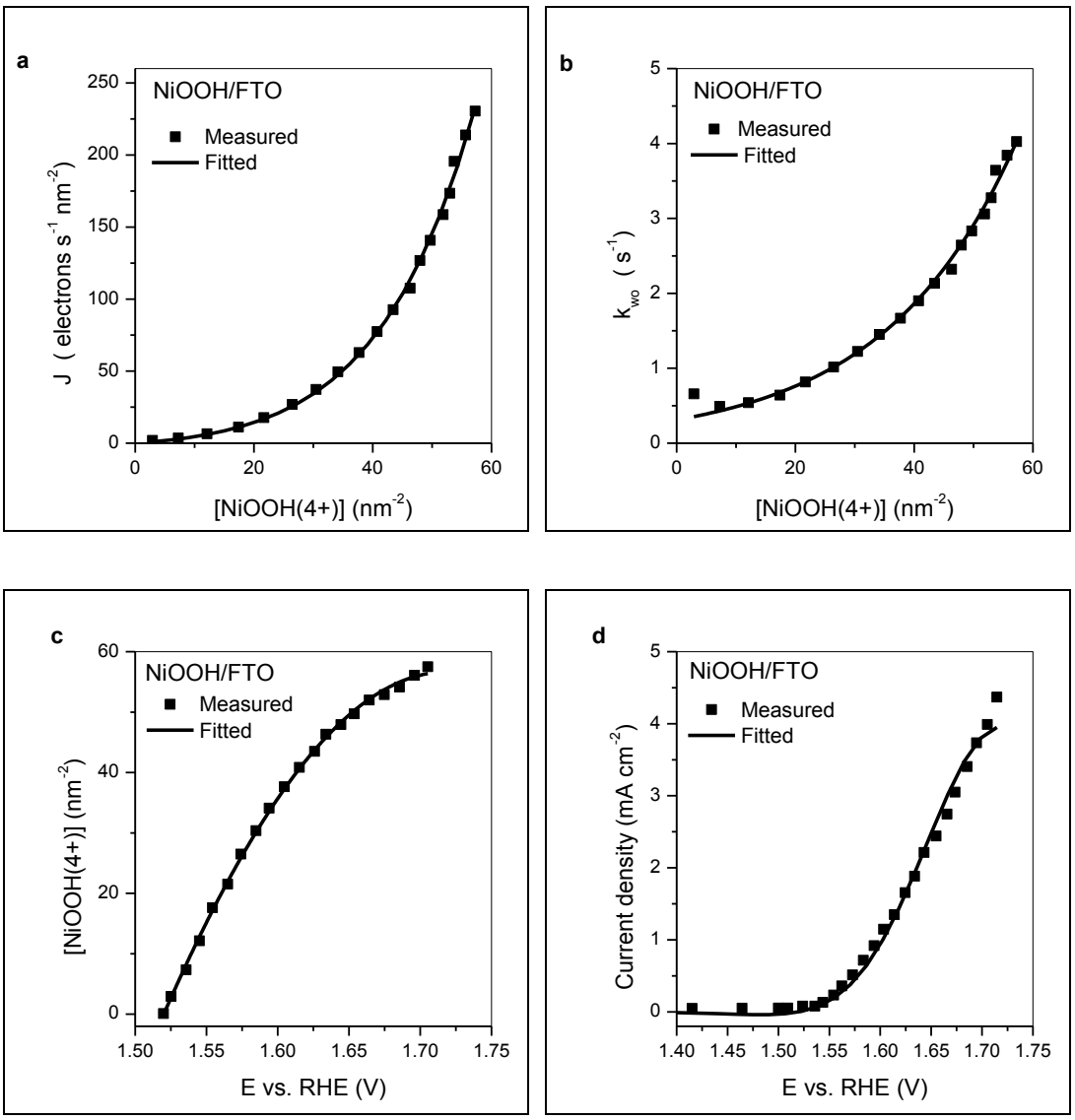

Supplementary Fig. 12 | Measured electrocatalytic response of NiOOH/FTO electrode. a, OER current density versus the concentration of NiOOH(4+) from spectroelectrochemistry, the data were from **Fig. 3a** in the Article[3] and fitted by **equation 3** in the main text (with result $i = 0.281859 \times \exp(0.046648 \times Q) \times Q$). **b**, Corresponding relationship between $\mathrm{OER\,current}/[\mathrm{NiOOH(4+)}]$ (or $\boldsymbol{k_{wo}}$) and $[\mathbf{NiOOH(4+)}]$ with fitting result $k_{wo} = 0.31126 \times \exp(0.04472 \times Q)$, R^2 = 0.992. c**,** The concentration of NiOOH(4+) vs. *i*R corrected potential from spectroelectrochemistry, the data were from Supplementary Fig. 11b in the Article[3] and fitted by **equation 4** in the main text (with result $Q = -494.92 + 551.58 \times \exp[-((x - 1.719)/0.60435)^2]$). **d**, OER current density versus *i*R corrected potential, the data were from **Supplementary Fig. 11b** in the Article[3] and fitted by **equation 5** in the main text (with result $i = 0.004964 \times \exp[0.046665 \times Q(E)] \times Q(E)$, $Q(E)$ parameters see **Fig. c).**

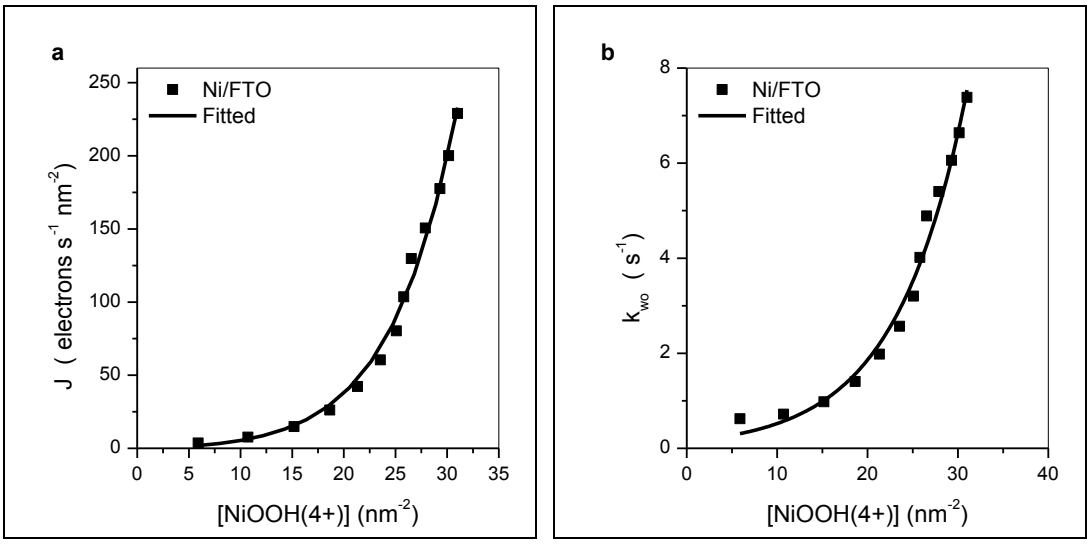

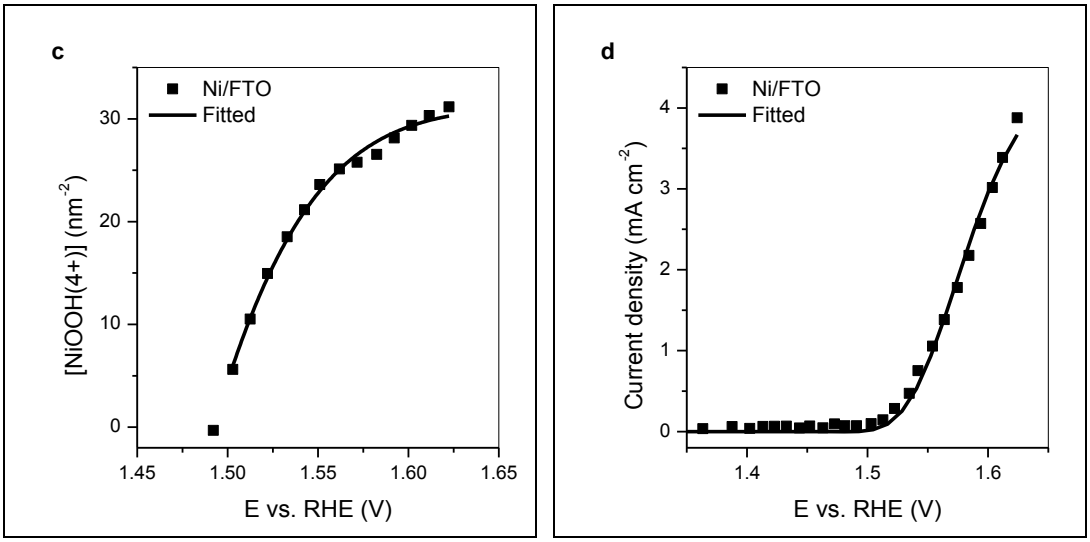

Supplementary Fig. 13 | Measured electrocatalytic response of Ni/FTO electrode. **a**, OER current density versus the concentration of NiOOH(4+) from spectroelectrochemistry, the data were from **Fig. 3a** in the Article[3] and fitted by **equation 3** in the main text (with result $i = 0.152998 \times \exp(0.125591 \times Q) \times Q$). **b**, Corresponding relationship between OER current/[NiOOH(4+)] (or $\boldsymbol{k_{wo}}$) and [NiOOH(4 +)] with fitting result $k_{wo} = 0.1461 \times \exp(0.12718 \times Q)$, R^2 = 0.984. **c**, The concentration of NiOOH(4+) vs. *i*R corrected potential from spectroelectrochemistry, the data were from **Supplementary Fig. 11a** in the Article[3] and fitted by **equation 4** in the main text (with result $Q = 31.364 - 206.96 \times \exp[-((x - 1.2962)/0.14175)^2]$). **d**, OER current versus *i*R corrected potential, the data were from **Supplementary Fig. 11a** in the Article[3] and fitted by **equation 5** in the main text (with result $i = 0.000895818 \times \exp[0.1615 \times Q(E)] \times Q(E)$, $Q(E)$ parameters see **Fig. c**).

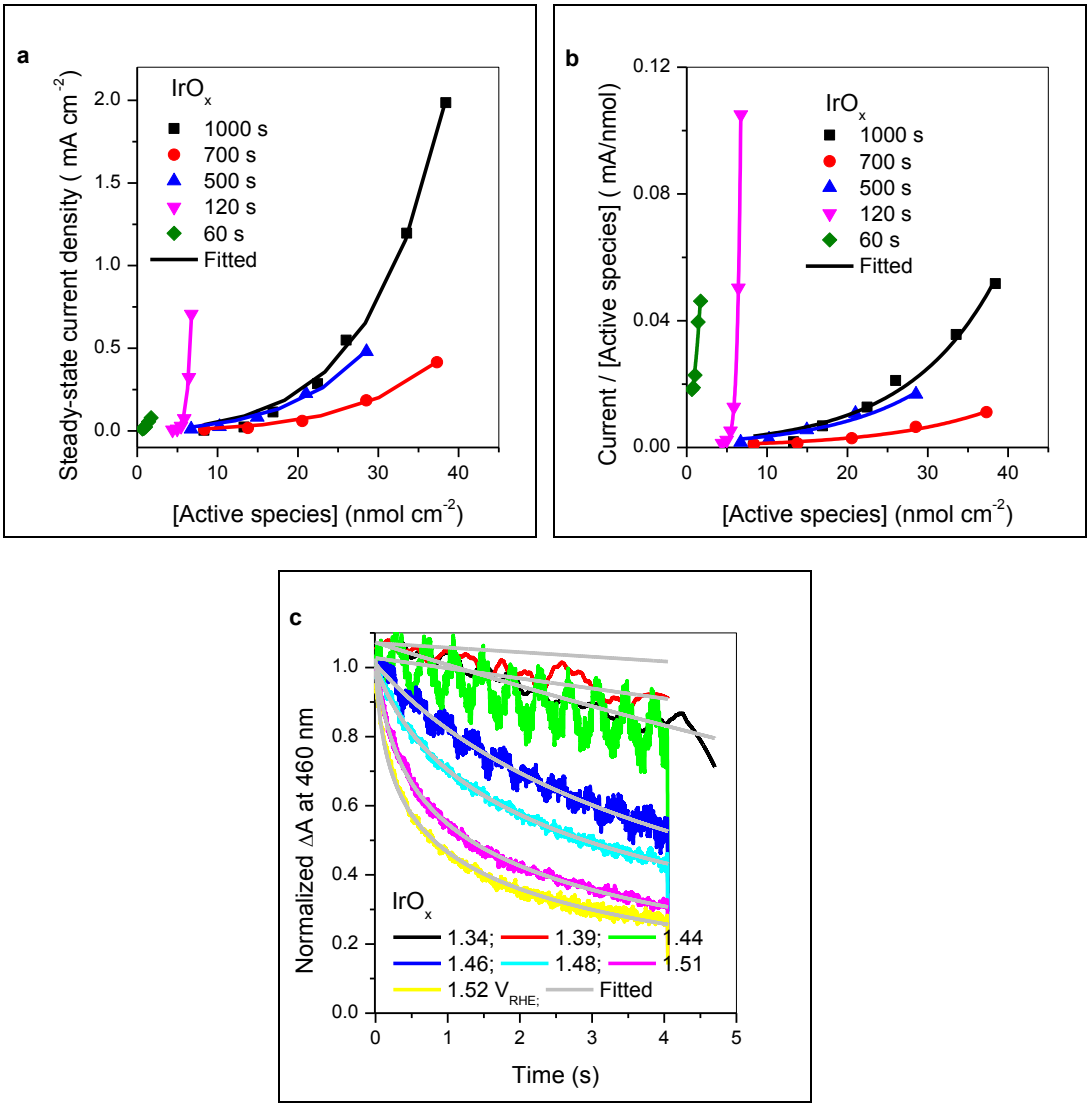

Supplementary Fig. 14 | Measured electrocatalytic response of IrO_x/FTO. a, Steady-state current plotted against the concentration of active species in IrO_x samples with different electrodeposition times (1000s, 700s, 500s, 120s and 60s), the data were from **Supplementary Fig. 11** in the Article[4] and fitted by **equation 3** in the main text (with results listed in **Table S15). b**, Corresponding relationship between **OER current/[active species]** (or $\boldsymbol{k_{wo}}$) and the concentration of active species with fitting results listed in **Table S16**. **c**, Absorption decay after turning the potential off, the data were from **Fig. 3a** in the Article[4] and fitted by **equation 3** in the main text (with result listed in

Table S17). IrO_x in 0.1 M $HClO_4$ water at pH 1.2.

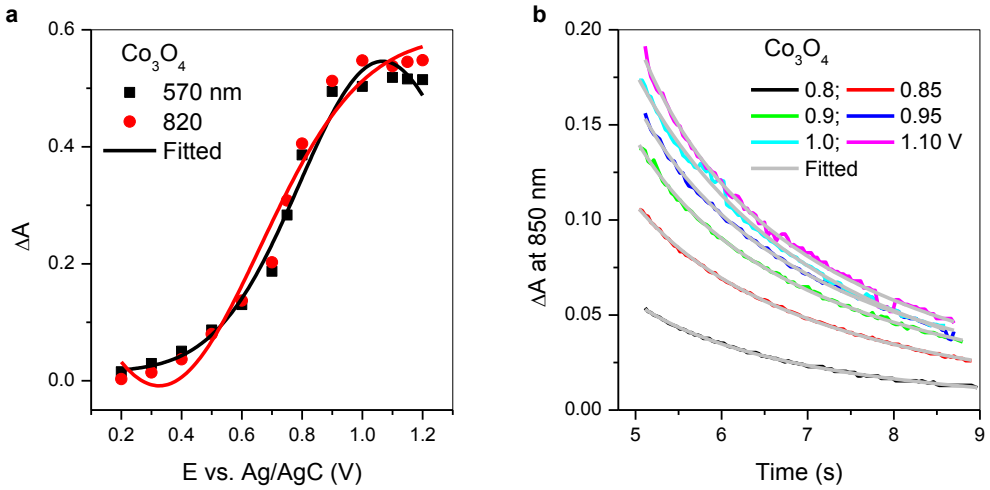

Supplementary Fig. 15 | Potential and corresponding accumulated charge decay for Co_3O_4 electrode. a, Absorption amplitude changes at 570 and 820 nm in *in situ* electrochemical UV-vis spectra against applied potential, the data were from **Fig. S7** in the Article[5] and fitted by **eq 4**. **b**, Optical data at 850 nm obtained from step-potential electro-induced absorption at high potential of 0.80 V to 1.10 V *vs* Ag/AgCl (Co^{3+}/Co^{4+} oxidation region) with 0.75 V *vs* Ag/AgCl as low potential (baseline) and fitted by **eq 3** in the main text. The origin data were from **Supplementary Figure S9** (**d**) in the Article[5].

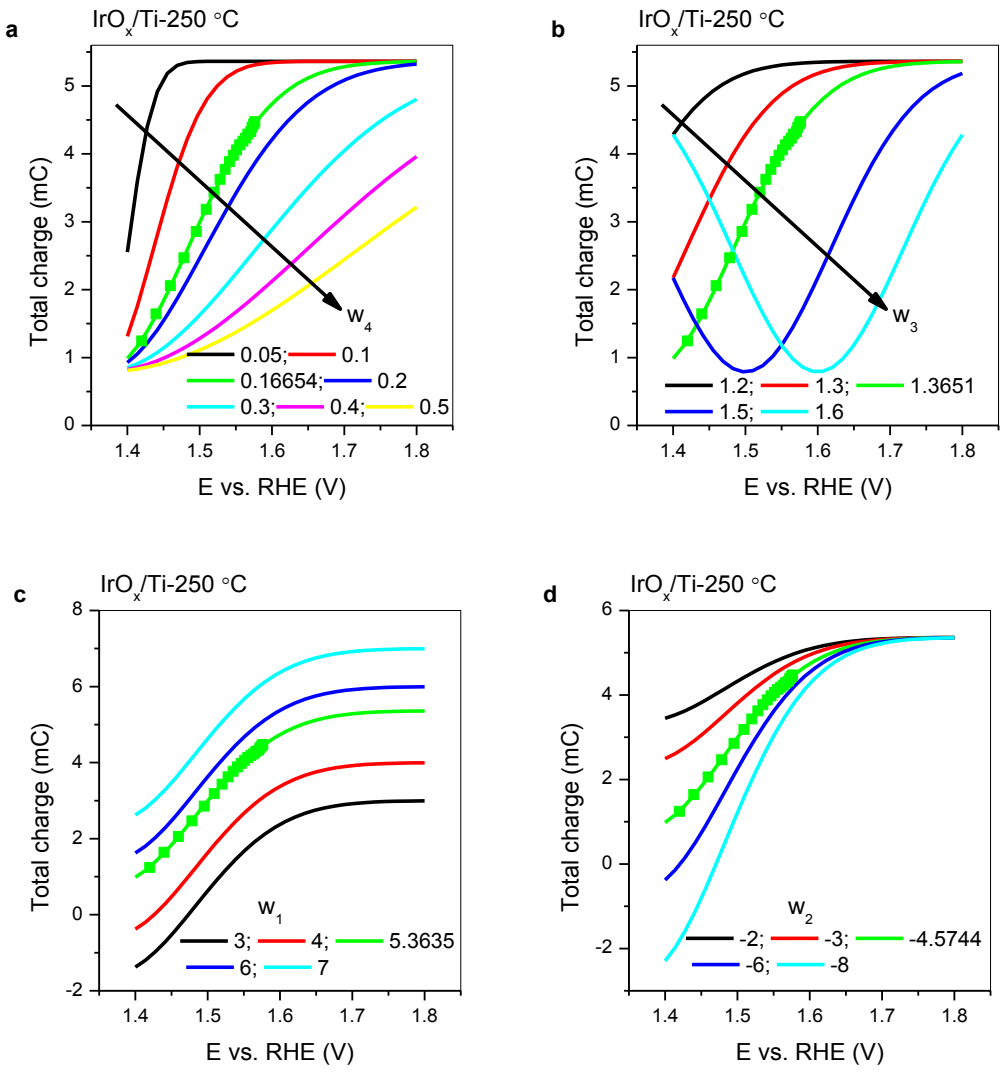

Supplementary Fig. 16 | Simulation of equation 4 in the main text. a, variation of parameter w_4, the green square scatter data were from **Fig. 1c** in the Article[1] and fitted by **equation 4** with result $Q = 5.3635 - 4.5744 \times \exp[-((x - 1.3651)/0.16654)^2]$, from which parameters w_1-w_3 are taken for simulation, kept constant and just varying parameter w_4. **b**, variation of parameter w_3, others are same as **Fig. a. c**, variation of parameter w_1, others are same as **Fig. a**. **d**, variation of parameter w_2, others are same as **Fig. a.**

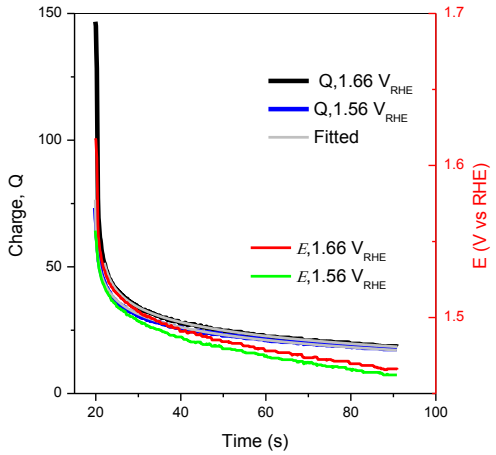

Supplementary Fig. 17 | Potential and corresponding accumulated charge decay for $Fe_{0.1}Ni_{0.9}O$ electrode. Measurement was conducted for the first 10 seconds, a potential of 1.45 V_{RHE} was applied. Between 10 and 20 seconds, a potential of 1.56 V_{RHE} (green trace) and 1.66 V_{RHE} (red trace) was applied. After 20 seconds, the measurement configuration was switched to open circuit (zero current density) and the potential decay was recorded, and this decay was converted to charge decay according to **eq 4** in the main text and then fitted by **eq 3** in the main text. The origin data were from **Supplementary Figure S11** in the Article[2].

Supplementary Tables

Table S1. Gauss fitting parameters for H_2O and H_2O_2 oxidation on IrO_x electrodes[a].

Probe wavelength (nm)	H_2O				H_2O_2			
	w_1	w_2	w_3	w_4	w_1	w_2	w_3	w_4
460	-0.03504	0.042728	1.5826	0.29677	0.054779	-0.05451	1.0429	0.46254
500	0.14237	-0.14314	1.2854	1.2297	-	-	-	-
550	0.1299	-0.13059	1.29	1.2665	-	-	-	-
600	0.000167	0.005397	1.5887	0.09784	-0.0098	0.039288	1.6473	0.49821
800	0.063945	-0.06452	1.2757	0.86022	-0.00388	0.048809	1.5436	0.30068
a-fit equation is **equation 4** in the main text.								

Table S2. *i-E* curve fitting parameters for H_2O and H_2O_2 oxidation on IrO_x electrodes[a].

Probe wavelength (nm)	H_2O		20 mM H_2O_2	
	k_0	A	k_0	A
460	0.020635	1088.59	10.8946	16.8224
500	0.401423	882.832	-	-
550	0.582936	1033.98	-	-
600	0.822643	945.32	7.22723	48.1676
800	0.227985	991.508	5.54986	23.2735
a-fit equation is **equation 5** in the main text, other fitted parameters see **Table S1**.				

Table S3. Gauss fitting parameters for water oxidation on FeOOH, FeOOHNiOOH and Ni(Fe)OOH electrodes[a].

electrodes	w_1	w_2	w_3	w_4
FeOOH	430.4	-431.37	0.29877	0.34602
FeOOHNiOOH	-11.594	557.38	0.63761	0.20104
Ni(Fe)OOH	50.36	-48.783	0.20605	0.19618

a-fit equation is **equation 4** in the main text.

Table S4. *i-E* curve fitting parameters for water oxidation on FeOOH, FeOOHNiOOH and Ni(Fe)OOH electrodes[a].

electrodes	k_0	A
FeOOH	0.000413	0.08015
FeOOHNiOOH	0.000197	0.034733
Ni(Fe)OOH	$5.93*10^{-5}$	0.201385

a-fit equation is **equation 5** in the main text, other fitted parameters see **Table S2**.

Table S5. Absorption decay curve fitting parameters for water oxidation on IrO_x electrodes[a]

Potential	$(\Delta A)_0$	k_0	A
1.27	1.0205	0.001229	4.1009
1.37	0.97951	0.42779	-2.0357
1.42	0.99878	0.17004	-7.4755
1.47	1.0513	0.001321	4.4057
1.51	1.0542	0.044068	2.5536
1.53	1.0674	0.051599	3.5929
1.55	1.0809	0.046114	4.2046
1.59	1.0653	0.093769	3.3477
a-fit equation is **equation 3** in the main text.			

Table S6. Absorption decay curve fitting parameters for water oxidation with H_2O_2 on IrO_x electrodes [a]

Potential	$(\Delta A)_0$	k_0	A
1.25	1.0223	0.13131	0.78504
1.32	1.0155	0.1445	0.81638
1.39	1.0096	0.085745	1.1108
1.44	1.0086	0.063353	1.3936
1.48	1.0087	0.04417	1.5697
1.52	1.0073	0.035508	1.7875
1.55	0.99844	0.050858	1.0508
1.58	0.98826	0.040767	1.0852
a-fit equation is **equation 3** in the main text.			

Table S7. *i-Q* curve fitting parameters for water oxidation on IrO_x/Ti electrodes at various rotation speeds[a].

Rotation speed (rpm)	k_0	A
800	0.000162	2.40839
1200	0.000217	2.36382
1600	0.000186	2.3375
2000	0.000233	2.29833
a-fit equation is equation 3 in the main text.		

Table S8. k_{wo}-*Q* curve fitting parameters for water oxidation on IrO_x/Ti electrodes at various rotation speeds[a].

Rotation speed (rpm)	k_0	A	R^2
800	1.68×10^{-4}	2.39978	0.99953
1200	1.08×10^{-4}	2.53125	0.999
1600	1.26×10^{-4}	2.42845	0.99991
2000	1.38×10^{-4}	2.42052	0.99987
a-fit equation is an exponential function.			

Table S9. Gauss fitting parameters for water oxidation on IrO_x/Ti electrodes at various rotation speeds[a].

Rotation speed (rpm)	w_1	w_2	w_3	w_4
800	-0.0541	2.8666	1.6048	0.17639
1200	-0.19143	4.7096	1.6161	0.1814
1600	-0.5651	5.1925	1.6262	0.20303

2000	5.2731	-4.5949	1.3534	0.17647

a-fit equation is equation 4 in the main text.

Table S10. *i*-*E* curve fitting parameters for water oxidation on IrO_x/Ti electrodes at various rotation speeds[a].

Rotation speed (rpm)	k_0	A
800	0.005595	2.57611
1200	0.003118	1.70396
1600	0.003596	1.62156
2000	0.002793	1.69296

a-fit equation is equation 5 in the main text, other fitted parameters see Table S3.

Table S11. *i*-*Q* curve fitting parameters for water oxidation on doped nickel oxides[a].

Doped element	k_0	A
Undoped	0.044617	0.012899
Zn	0.0036	0.0106
Fe	0.187954	0.00968296
Co	0.035817	0.0075891
Mn	0.0103	0.0049

a-fit equation is equation 3 in the main text.

Table S12. k_{wo}-*Q* exponential fitting parameters for water oxidation on doped nickel oxides[a].

Doped element	k_0	A	R^2

Undoped	0.04589	0.01245	0.94221
Zn	0.00701	0.00789	0.83094
Fe	0.16782	0.01089	0.94445
Co	0.03269	0.00804	0.99346
Mn	0.01197	0.00437	0.9627

a-fit equation is equation 3 in the main text.

Table S13. Gauss fitting parameters for water oxidation on doped nickel oxides[a].

Doped element	w_1	w_2	w_3	w_4
Undoped	-68.063	174.37	1.959	0.35993
Zn	-319.81	579.23	1.9243	0.34814
Fe	714.17	-726.85	1.4236	0.47226
Co	1455.8	-1475.7	1.4663	0.43052
Mn	562.6	-669.33	1.4312	0.17227

a-fit equation is **equation 4** in the main text.

Table S14. *i-E* curve fitting parameters for water oxidation on doped nickel oxides[a].

Doped element	k_0	A
Undoped	0.000735	0.013054
Zn	6.29×10^{-5}	0.010821
Fe	0.002704	0.018975
Co	0.000488	0.009624
Mn	0.0002	0.0054

a-fit equation is equation 3 in the main text.

Table S15. *i*-*Q* curve fitting parameters for water electrooxidation on IrO_x/FTO[a].

Time (s)	k_0	A
1000	0.002277	0.081485
700	0.00079	0.071123
500	0.00206	0.073947
120	1.93×10^{-7}	1.95772
60	0.010165	0.894311

a-fit equation is equation 3 in the main text.

Table S16. k_{wo}-*Q* exponential fitting parameters for water electrooxidation on IrO_x/FTO[a].

Time (s)	k_0	A	R^2
1000	0.00171	0.08948	0.97698
700	6.24×10^{-4}	0.07776	0.98269
500	0.00149	0.08597	0.95625
120	7.39×10^{-9}	2.44847	0.99964
60	0.00936	0.94772	0.95055

a-fit equation is equation 3 in the main text.

Table S17. Absorption decay curve fitting parameters for water electrooxidation on IrO_x/FTO[a].

Potential	$(\Delta A)_0$	k_0	A
1.34	1.0725	0.076171	-0.19519
1.39	1.0705	0.064736	-1.5643
1.44	1.0274	0.063145	-0.76058
1.46	1.0094	0.059217	1.3708
1.48	1.0028	0.034423	2.7963
1.51	1.025	0.041385	3.7331
1.52	0.99159	0.043205	4.3976

a-fit equation is **equation 3** in the main text.

Supplementary References

1 Nong, H. N. *et al.* Key role of chemistry versus bias in electrocatalytic oxygen evolution. *Nature* **587**, 408-413, doi:10.1038/s41586-020-2908-2 (2020).

2 Rao, R. R. *et al.* Spectroelectrochemical Analysis of the Water Oxidation Mechanism on Doped Nickel Oxides. *J. Am. Chem. Soc.* **144**, 7622-7633, doi:10.1021/jacs.1c08152 (2022).

3 Yuan, Y. *et al.* Kinetics of Active Oxide Species Derived from a Metallic Nickel Surface for Efficient Electrocatalytic Water Oxidation. *ACS Energy Letters* **7**, 3276-3285, doi:10.1021/acsenergylett.2c01493 (2022).

4 Bozal-Ginesta, C. *et al.* Spectroelectrochemistry of Water Oxidation Kinetics in Molecular versus Heterogeneous Oxide Iridium Electrocatalysts. *J. Am. Chem. Soc.* **144**, 8454-8459, doi:10.1021/jacs.2c02006 (2022).

5 Kang, W. *et al.* Unraveling Sequential Oxidation Kinetics and Determining Roles of Multi-Cobalt Active Sites on Co_3O_4 Catalyst for Water Oxidation. *J. Am. Chem. Soc.* **145**, 3470-3477, doi:10.1021/jacs.2c11508 (2023).